MEASUREMENT OF THE THERMAL PERFORMANCE OF A BOREHOLE HEAT EXCHANGER WHILE INJECTING AIR BUBBLES IN THE GROUNDWATER

EDUARD CALZADA OLIVERAS

Master of Science Thesis

Stockholm, Sweden 2012

Measurement of the thermal performance of a Borehole Heat Exchanger while injecting air bubbles in the groundwater

Eduard Calzada i Oliveras

	Master of Science Thesis EGI 2012:048MSC	
KTH Industrial Engineering and Management	**Measurement of the thermal performance of a Borehole Heat Exchanger while injecting air bubbles in the groundwater**	
	Eduard Calzada i Oliveras	
Approved	Examiner Björn Palm	Supervisor José Acuña
	Commissioner	Contact person

Abstract

The most common way to exchange heat with the ground in Ground Source Heat Pump (GSHP) applications is with borehole heat exchangers (energy collectors in vertical wells). These boreholes contain the pipe with the secondary fluid of the GSHP and they are often filled with natural groundwater. It has been recently discovered that injecting air bubbles in the groundwater side of the boreholes increases the efficiency of the heat transfer. The aim of this thesis is to analyze the thermal changes in the borehole and the surrounding ground when bubbles are injected in the groundwater. Experiments are carried out through a distributed thermal response test along the borehole using two different rates of bubble injection. Temperature profiles of the secondary fluid and the groundwater are analyzed and calculations on the thermal resistances inside the borehole and the conductivity of the ground are made. Moreover, the validity of the line source conduction model is discussed under the above mentioned circumstances.

Acknowledgements

Table of Contents

Index of Figures

Index of tables

Objectives

This project aims at analyzing the heat transfer changes when air bubbles are injected in the groundwater side of a borehole heat exchanger. The major objective of this thesis is to investigate how much heat transfer parameters are enhanced along the borehole depth.

Specifically, the objectives are:

1. Analysis of the bubble flow rate and the bubble velocity inside the groundwater.

2. Qualitative study of temperature profiles during bubble injection.

3. Quantitative comparison of the borehole resistance values along the depth with bubble injection in contrast to normal conditions.

4. Feasibility study on using the line source model when the bubbles are injected.

5. Analysis of the thermal behaviour of the rock along the depth. Quantification of a representative value of the effective rock conductivity in contrast to normal conditions.

6. Study of the relation between bubble flow rate, thermal performance and injection costs.

7. Analysis of the relation between the depth of the injection point and the increase of the heat transferring conditions.

8. Preliminary study of the evolution of the convection coefficient between the groundwater and the surrounding walls (pipe and borehole wall) during bubble injection.

Methodology

The project has been structured in three consecutive phases:

Literature survey:

- A theoretical research of the project field. The most relevant bibliography is summarized and used to make assumptions and calculations in the analysis of the results.
- A research of recent studies related to the specific topic, especially previous work carried out by (Acuña J. , 2010) and (Kharseh, 2010) in borehole heat exchangers.

Experimental work:

- Preliminary tests in the borehole heat exchanger to properly address the main experiment of the project.
- Distributed Thermal Response Test (DTRT) of the borehole heat exchanger in heating conditions with the presence of bubbles in the groundwater side.

Analysis:

- Qualitative analysis of the data obtained in both preliminary tests and the DTRT in relation with heat transfer theory.
- Quantitative analysis of the thermal borehole Resistance and the conductivity of the Rock.

The experiments have been carried out in a groundwater filled borehole of the KTH experimental installation in the south of Stockholm.

This project has been written between the months of January and June 2012 in Stockholm, Sweden.

1 Introduction

1.1 Ground source heat pumps

Ground source heat pumps (GSHP) transfer heat from or to the surface of the Earth through a series of fluid-filled and buried pipes. They work differently depending on the season. In winter they collect heat from the warmer soil. In summer, the soil temperature is cooler than the outside air, and the GSHP is then reversed to provide an element of cooling.

Secondary
fluid (blue)

Groundwater
(yellow)

Ground/Rock
(white)
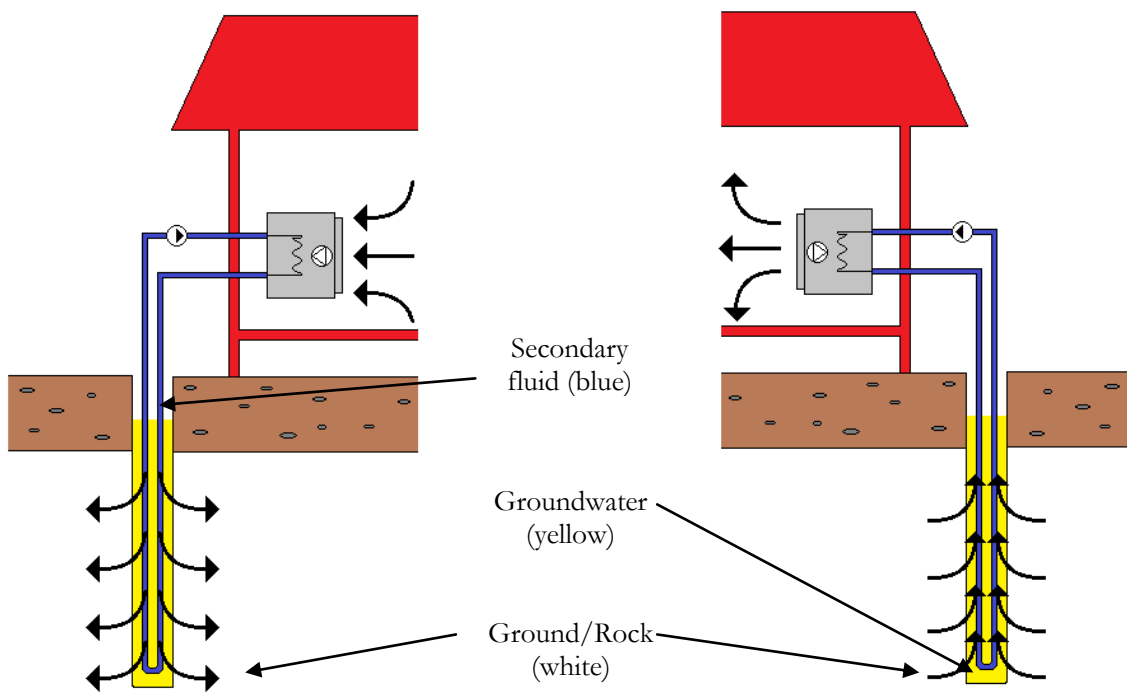
Figure 1: Borehole heat exchanger cooling in summer (left) and heating in winter (right)

A GSHP includes three principle components—an earth connection subsystem, a heat pump subsystem, and a heat distribution subsystem. This thesis will essentially study the earth connection subsystem that usually includes a closed loop of pipes that are buried vertically. A fluid circulates through these pipes, allowing heat but not fluid to be transferred from the building to the ground or vice versa. The circulating fluid is generally water or a water/antifreeze mixture. (Omer, 2008)

In a borehole heat exchanger, plastic pipes (polyethylene or polypropylene) are installed in boreholes, and the remaining room in the hole is usually filled with natural groundwater. The borehole studied in this thesis is a U-pipe type, consisting of a pair of straight pipes, connected by a 180° turn at the bottom. A big advantage of the U-pipe is low cost of the pipe material, resulting in double U pipes being the most frequently used borehole in Sweden. (Omer, 2008)

1.2 Current situation of the GSHP technology in Europe and motivations for doing this thesis

The climatic conditions in central and northern Europe have basically a demand for space heating; air conditioning is rarely requested. Therefore heat pumps in Europe usually operate in heating mode. However, with the inclusion of larger commercial applications that require cooling, and the ongoing proliferation of the technology into Southern Europe, the double use for heating and cooling is becoming more important.

In fact, significant growth rates can be observed and today's total number of GSHP systems in Europe is roughly about 1.25 million, mainly used for residential space heating. Moreover, Sweden concentrates about one third of these systems in Europe. Heat pump manufacturers report that 97% of newer Swedish houses are built with ground source heat pumps (Bayer, 2012). The worldwide number of GSHPs is rapidly growing, and GSHPs are gaining more importance, especially in Europe. This is stimulated by the search for environmental alternatives to traditional heating technologies, both for new and old buildings.

Nevertheless, air source heat pumps are recommended for mild and moderate climate regions, where winter temperatures usually remain above 0ºC (Sanner, 2003). In the Southern European countries, this source of energy still remains very unusual despite the optimal ground thermal conditions. The environmental friendly conditions have not convinced yet the population and the governments to establish a strong policy to promote the usage of GHSP's, possibly due to the big investment needed for the installation.

In my opinion, further knowledge on this technology will eventually imply a larger commercialization of the product. Explanations about the advantages (including the economical) on the GHSP will help to develop this technology in Southern European countries.

1.3 The bubble injector: Energy Booster

A bubble injector system patented by Willy Ociansson as the "Energy Booster" is used in this project. This system is based on the injection of bubbles in the groundwater side. It's been proved that the injection of bubbles in the groundwater enhance the heat transfer in a BHE (Kharseh, 2010). There is therefore an increase in the efficiency of the system.

Previous work has detected a reduction of the borehole thermal resistance and an increase in the conductivity of the ground (in average values). However, there is a lack of knowledge of where exactly the heat transfer conditions are being enhanced along the depth. Further learning of what is going on along the pipe will not only give a better understanding of the system but will also be a tool that will drive to conclusions and suggestions of how to optimize the usage of this system.

In my case, the system works as follows: the bubbles are made of nitrogen which is compressed in an air tank at a high pressure (up to 200 bars). The tank, located on the surface of the Earth, is linked to the groundwater with a pipe that goes deep into the borehole. The procedure to inject bubbles from the air tank to the groundwater is based on the pressure of the groundwater at the injection point: if the pressure of the nitrogen in the pipe is higher than the one in the groundwater (at the end of the pipe), the air will penetrate the water until the pressures are equal.

The pipe that links the tank with the groundwater is deepened into the water with the help of a weight that drags the pipe on the way down. Once decided the depth of the pipe, the pressure of

that point is calculated (based on how many meters of water there are above that point). In the output of the tank there is a pressurized valve that allows the output of compressed air at a specific indicated pressure. If the pressure marked in the valve is the same or higher than the groundwater at the end of the pipe, the air escapes and bubbles are formed in the groundwater. This way allows the introduction of the bubbles into the groundwater at a desired depth without any need of extra energy. The only cost in this injection is the value of the air compressed in the tank.

Moreover, there is a programmable relay in the output of the tank that lets the air through during a specific period of time, forming cycles with a determined period of air. The amount of bubbles and its size are then graduated.
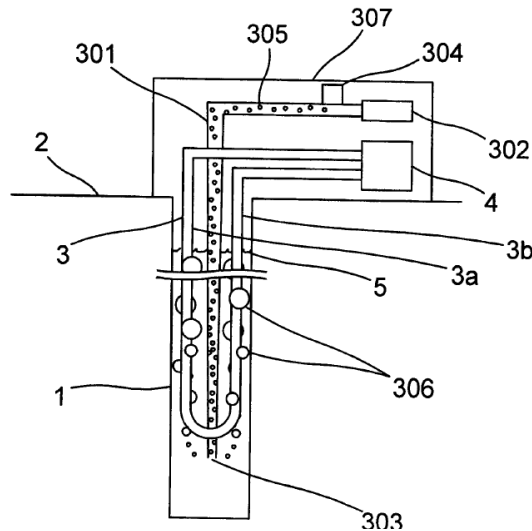
Figure 2: Energy Booster Patent (Ociansson, 2011)

Where:

5… groundwater level

302… air tank

303… weight

304… pressurized valve + programmable relay

To sum up, one has to decide in what depth the bubbles can be injected and the frequency and size of the bubbles. In fact, one of the aims of this thesis is to optimize the efficiency of the heat transfer in relation with the quantity of air spent.

1.3.1 Equation of state for the N2 bubbles

In order to make some calculations, an equation of state has to be used for the N2 of the tank. When considering the ideal gas equation of state a total lack of influence between the gas particles is implied. Therefore, given the high pressure conditions inside the tank the gas can't be considered ideal. In spite, various real gas equations were analysed.

The ideal gas treats the molecules of a gas as point particles that interact with each other with perfectly elastic collisions. This approximation works well for dilute gases in some experimental cir-

cumstances. But gas molecules are not point masses, and there are circumstances, such as when the pressures are medium-high (like in the experiment, at around 100 bar), where the properties of the molecules have an experimentally measurable effect. A modification of the ideal gas law was proposed by Johannes D. van der Waals in 1873 (Nave, 2005). This new equation took into account the molecular size and molecular interaction forces. It is referred to as the van der Waals equation of state:

$$P = \frac{R \cdot T}{v - b} - \frac{a}{v^2}$$

<div align="right">Eq. 1.1</div>

Where:

P… pressure of the gas

R… ideal gas constant

T… temperature of the gas

v… molar volume of the gas

The Van der Waals force consists on the molecular interaction between the particles that has a negative effect on the macroscopic pressure of the gas. It is referred in the equation in the term "$\frac{a}{v^2}$". This term involves the pressure constraint "a", which measures the specific strength of the interactions between the particles (Nave, 2005). While divided by the square of the specific volume, the term takes into account the density of the air: the denser the air is the higher is the Van der Waals interaction.

On the other hand, the equation contains a volume constant, "b", which is related to the "size" of the molecules or, in a refined statistical theory, to the intermolecular distance at which the attractive forces become strongly repulsive (Nave, 2005). The term "$v - b$" takes only into account the void space left in a determined volume.

The constants "a" and "b" have positive values and are characteristic of each individual gas. The van der Waals equation of state approaches the ideal gas law when the values of these constants approach the zero value. In the particular case of the N2, the values are the following:

<div align="center">
a= 1.3361 $\frac{dm^6 \cdot bar}{mol^2}$ b= 0,038577 $\frac{dm^3}{mol^2}$
</div>

1.4 State of the Art in the bubble injection technique

Mohamad Kharseh, a PhD for Luleå University of Technology, published in 2010 a paper (Kharseh, 2010) about the improvements of some thermal properties in a BHE while injecting bubbles in the groundwater, the only scientific work done so far about this technique.

He first stated that heat injection or extraction causes a temperature gradient in and around the borehole along the pipes, which induces convective flow in the groundwater. On the other hand, (Gustafsson & Gehlin, 2008) concluded that when comparing the usage of groundwater with stagnant water, there is a reduction of the borehole thermal resistance in the former. Moreover, in frac-

tured bedrock or high porosity ground material, convective flow may also influence the ground conductivity.

Due to the lack of a direct method to measure the thermal resistance, (Kharseh, 2010) used thermal response tests (TRT), a method to measure temperatures that allow calculations on the average heat parameters. This methodology can be summarized as follows. A circulation pump circulates a heat carrier (water or antifreeze-water) at constant flow rate between a heater with constant power rate and a vertical plastic pipe installed vertically in a borehole. The measured variables during the TRT, which are continuously logged, are the borehole incoming and outgoing temperatures, the outdoor temperature, the flow rate, and the heat injection power. Analyzing the evolution of these temperatures enables calculating the different parameters.

The analytical technique that (Kharseh, 2010) used to analyze the experiment data is based on Kelvin's line source theory (LSM). Explanations about the analytical technique can be found in chapter 1.8 of this report. It is remarkable that this model is based on purely conduction heat transfer through the ground, ignoring the convection between the groundwater and the rock outside the borehole.

The main conclusions extracted from these results were that the injection of bubbles at the bottom of the borehole reduces the thermal borehole resistance by 29.7 %, and the effective thermal conductivity is increased by 33.8%, showing the improvement of the geothermal heat pumps, in terms of the geothermal conditions in the borehole and in the ground. These values are average values for the borehole.

My work will start from this initial point. I will proceed by studying the heat transfer parameters in the borehole with a distributed thermal response test with heat injection, analyzing the thermal response along the borehole. With a division of the borehole length into sections, the thermal resistance in every section along the pipe will be calculated. Moreover, the test will provide a visualization of the temperature profiles in the groundwater and in the secondary fluid that will allow a comparison with the case without bubbles. Eventually, some suggestions might be made in order to optimize the energy spent with the bubbles (optimal locations of the bubble injection, optimal quantities of bubbles, etc.). Also, the convection coefficient between the bubbles groundwater will be studied.

1.5 Distributed Thermal Response Test

The temperature measurements are made in the secondary fluid and in the groundwater side along the depth every four meters. The measurement equipment is based on a fibre cable that uses the thermo sensitive dependence of the laser propagation through the cable to measure the temperature along the cable. In the experiments, the cable used is 1147 meters long. The first half of the fibre cable is introduced in the secondary fluid pipe to measure the temperature of the secondary fluid: it is first deepened from the top of the borehole until a depth of approximately 250 meters and then it goes up until the top, always inside the pipe. The second half is in contact with the groundwater, and it is also deepened until the bottom part of the borehole.

The working principle of the DTS technology is based on Raman optical time domain reflectometry. Pulses of laser light are injected through the length of an optical fiber. In the desired point, the laser light is reflected and re-emitted back through the fiber to the origin. What gives information about the temperature of the point is the detection of the non-linear part of the reflected light that is re-emitted with a different frequency than the input signal. This frequency shifted light scattering is called Raman scattering, and the temperature is determined by analyzing it over a peri-

od of time. Further information about the use of DTS technology in borehole heat exchangers can be read in the work of (Acuña J. , 2010).

1.6 Representation of the case study

A section of the borehole with the equivalent system installed is represented in Figure 3.

$$T_f - T_b = q \cdot R_b$$

$$T_b - T_g = q \cdot R_g$$
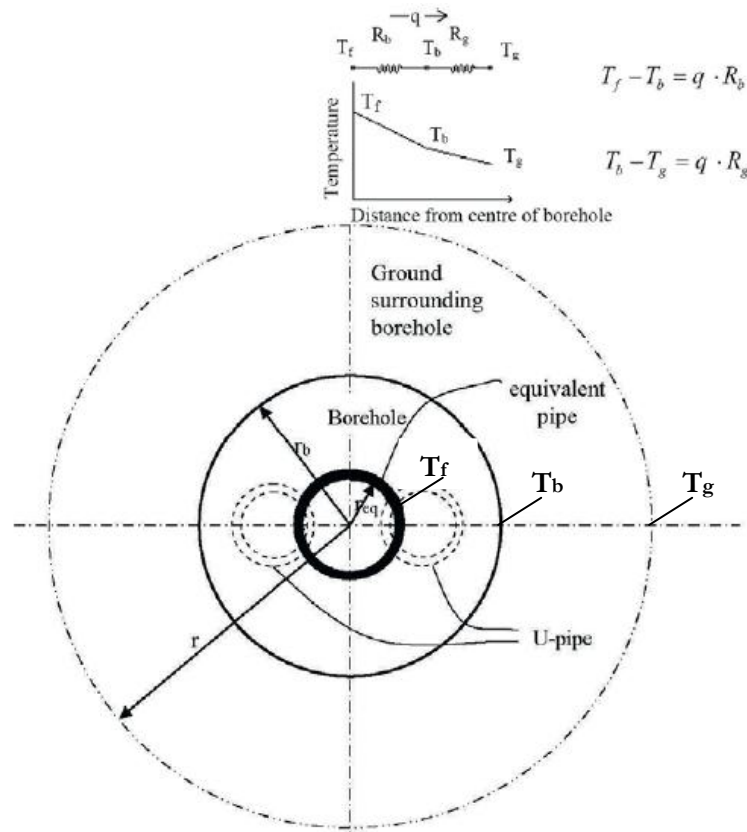
Figure 3: Representation of the case study (Kharseh, 2010)

Where:

T_f… temperature of the fluid, average value of the upwards and downwards direction

T_b… temperature of the borehole wall

T_g… temperature of the undisturbed ground

R_b… thermal borehole resistance

R_g… thermal resistance of the ground

First, the two pipes are simplified into an equivalent pipe. The temperature of the secondary fluid circulating in the pipe is T_f, an average of the fluid temperature in the way up and down at every specific depth.

By definition, the thermal resistance links the difference of temperatures between two points and the heat transferred between them. In a borehole, there is energy transferred from the secondary fluid (Tf) till the undisturbed ground (Tg). The resistance of the system is then:

$$Q = R \cdot (Tf - Tg) \hspace{3cm} \text{Eq. 1.2}$$

The resistance R can be divided in stretches:
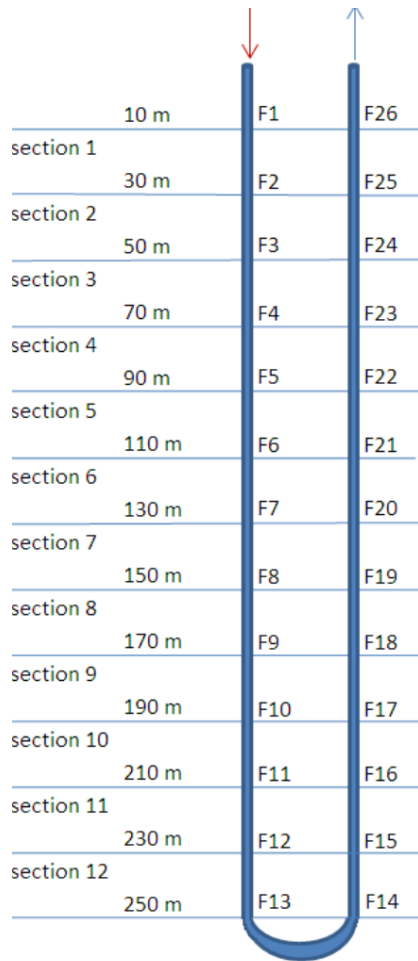
Rb1… Convection between the secondary fluid and the internal wall of the pipe.

Rb2… Conduction through the pipe.

Rb3… Convection between the external wall of the pipe and the groundwater.

Rb4… Effect of conduction through the groundwater.

Rb5… Convection between the groundwater and the borehole wall.

Rrock… Conduction through the surrounding ground.

The total resistance between the secondary fluid and the undisturbed groundwater is divided into the resistance of the borehole and the resistance of the rock:

$$R = Rb + Rrock \hspace{3cm} \text{Eq. 1.3}$$

Where the thermal resistance of the borehole is defined as follows:

$$Rb = Rb1 + Rb2 + Rb3 + Rb4 + Rb5 \hspace{2cm} \text{Eq. 1.4}$$

The resistances that are expected to be reduced with the injection of bubbles are Rb3 and Rb5, as well as Rrock (as presented in (Kharseh, 2010), due to the enhancement of the convection.

Depth	Down	Up
10 m	F1	F26
section 1		
30 m	F2	F25
section 2		
50 m	F3	F24
section 3		
70 m	F4	F23
section 4		
90 m	F5	F22
section 5		
110 m	F6	F21
section 6		
130 m	F7	F20
section 7		
150 m	F8	F19
section 8		
170 m	F9	F18
section 9		
190 m	F10	F17
section 10		
210 m	F11	F16
section 11		
230 m	F12	F15
section 12		
250 m	F13	F14

Figure 4: Borehole divided in sections (Acuña J. , 2010)

On the other hand, in most of the quantitative analysis the depth of the borehole is divided into 12 sections. Figure 4 shows this division, the same one done by (Acuña J. , 2010). The borehole is around 260 meters depth, and it is divided into 12 sections of 20 meters each. The first ten meters of pipe as well as the last 10 meters are excluded of the numerical study. Each section has one stretch of the pipe on its way up and another on its way down.

Finally, it is important to point out that points F1 and F6 are located 10 meters below the groundwater level. Therefore, all the temperature profiles shown in this report consider the origin (meter 0) on the groundwater level, instead of the ground level.

1.7 Convection

If we consider a fluid of velocity V and temperature T_{ext} flowing over a surface of area A and temperature T_s, in the case of $T_{ext} \neq T_s$, convection heat transfer will occur. The relation of the differ-

ence of temperatures between the surface and the fluid with the local heat flux (Q'') can be expressed as (Incropera, 2007):

$$Q'' = h'' \cdot (Ts - Text)$$

Eq. 1.5

Where *"h"* is the local convection coefficient that relates heat and temperatures locally. Due to the fact that conditions vary from point to point on the surface the coefficient also varies. Therefore, we can consider the average value of the coefficient by integrating along the surface:

$$h = \frac{1}{A} \cdot \int h'' \cdot dA$$

Eq. 1.6

The total heat transfer rate is then:

$$Q = h \cdot A \cdot (Ts - Text)$$

Eq. 1.7

It is therefore of great importance to obtain the value of the coefficient *h* to evaluate the importance of the convection heat transfer in the whole process of energy transfer.

1.7.1 Forced convection

This thesis focuses on the improvement of heat transfer with bubbled groundwater, a problem with low speed forced convection and with no phase changing occurring within the fluid. Although no phase change takes place, it is a two-phase flow problem. In the bubble injection process, the convection is enhanced in a non-natural way.

In order to determine convection parameters, two approaches can be considered: the theoretical and the experimental. The theoretical approach consists on solving the boundary layer equations of the geometry studied. Obtaining a temperature profile is then used to evaluate the Nusselt number in a proper correlation and therefore the local convection coefficient *"h"* can be calculated. Integrating along the x axis, an average value of *"h"* is obtained. Experimentally, measuring the temperatures of the two substances in contact and with equation 1.5, the *"h"* coefficient can be calculated.

1.7.2 The thermal boundary layer

When there is a flow over a surface, a velocity boundary layer appears: it consists on an area with lower fluid velocity due to the contact of the fluid with the surface. The velocity of the fluid in contact with the surface is zero (equilibrium), and it increases, until it reaches the global flow speed. This gradient of speeds along the layer involves friction between the flow particles.

Thermally, if the fluid stream and surface temperature differ, a thermal boundary layer develops. The similarities with the velocity layer are numerous. Fluid particles in contact with the surface achieve thermal equilibrium and thus the same temperature T_s. At the same time, this particles exchange energy with those in the adjoining fluid layer. This energy transfer involves a gradient of temperatures. The region where this gradient exists is called the thermal boundary layer (Incropera, 2007).

An important step previous to any analysis of the convection is to determine whether the boundary layer is laminar or turbulent. The *"h"* convection coefficient depends on what are the conditions of the layer.

In a laminar boundary layer, fluid motion is ordered and streamlines where particles move along can be easily identified. The shape of the temperature diagram is smoothly curved. However, in a turbulent layer, fluid motion is very irregular and has velocity fluctuations that enhance the transfer of energy. This involves a stronger change of temperature along the layer and thus a more curved temperature diagram (Incropera, 2007).

In terms of reducing the thermal resistance of the borehole (between the secondary fluid and the internal walls of the pipes), the turbulent flow is desired. However, the energy required in the pump to induce turbulence must be regulated so that the energy consumption is optimized in terms of overall energy cost. The pumping power is proportional to the pressure drop ΔP, which mainly happens due to friction, whose value strongly depends on the velocity of the fluid.

1.7.3 Parameters: Reynolds, Nusselt and Prandtl numbers

The Reynolds number defines if the type of flow is laminar or turbulent. It is defined by a dimensionless grouping of variables:

$$Re = \frac{V \cdot Dh}{v} \qquad \text{Eq. 1.8}$$

With:

V… velocity of the fluid

Dh… hydraulic diameter

v… cinematic viscosity of the fluid

The Reynolds number can be interpreted as a ratio of the inertial and viscous forces. The critical Reynolds number where the flow changes from laminar to turbulent varies from 2300 to 4000. Below this margin the flow is considered laminar and above is turbulent (Incropera, 2007).

The Nusselt number is a parameter that can be equaled to the dimensionless temperature gradient at the surface, and it measures the convection heat transfer occurring at the surface.

$$Nu = \frac{dT}{dy} = \frac{h \cdot Dh}{\lambda} \qquad \text{Eq. 1.9}$$

With:

λ… conductivity of the water

The Nusselt number represents the gradient of dimensionless temperatures on the surface. (Incropera, 2007) However, the Nusselt number is to the thermal boundary layer what the friction coefficient is to the velocity layer.

Finally, the Prandtl number is a ratio between the momentum and energy diffusivity, and also dimensionless:

$$Pr = \frac{\mu \cdot Cp}{\lambda} \qquad \text{Eq. 1.10}$$

Where:

μ… Dynamic viscosity

C$_P$… specific heat

1.7.4 "h" convection coefficient: Nusselt correlation

A theoretical value of the "h" coefficient can be calculated through the heat transfer parameters. There are several equations suggested to find the Nusselt number, which depend on the fluid in contact with the wall. These equations are generally obtained experimentally, approximating the correlation to the data obtained. There are a number of correlations already invented, and in the case of the bubbled groundwater some assumptions need to be done to use any of them, as the case of bubbled groundwater has never been studied. The fluid is a two flow phase: water and air (nitrogened air) and the equation considered is the Groothuis and Handel two-phase flow correlation:

$$Nu = 0,029 \cdot Re^{0,87} \cdot Pr^{\frac{1}{3}} \cdot \left(\frac{\mu b}{\mu w}\right)^{0,14} \qquad with\ Re > 5000 \qquad \text{Eq. 1.11}$$

The Groothuis and Handel correlation can only be used for water-air flow in vertical tubes. The fluid has to be turbulent and the relation of volumes between the air and the water should be 1-250.

The results of their measurements are considered to be satisfactory in the indicated conditions (Kim, 2002), and they are plotted in the following Figure:
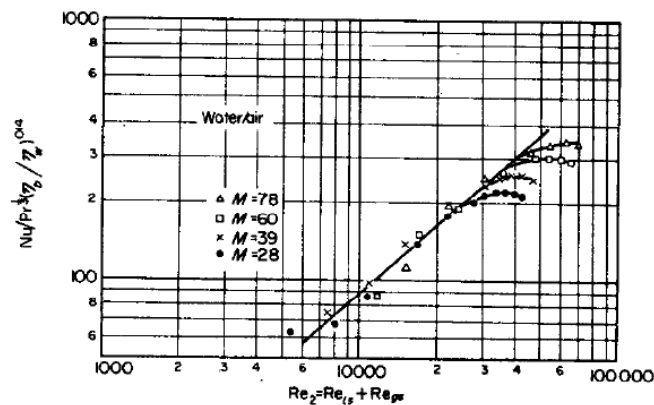
Figure 5: Correlation of heat transfer data for the two phase water/air (Groothuis & Hendal, 1959)

Where:

μb…viscosity of the liquid in the bulk

μw… viscosity of the fluid in the wall temperature

One assumption done when using this correlation in the case study is that the temperature conditions in the radial direction are constant. As μ is basically function of the temperature (and needs big temperature differences to change considerably), the expression $\left(\frac{\mu b}{\mu w}\right)^{0,14}$ is thus equaled to one.

19

The physical properties mainly depend on the temperature (and in a lower scale on the pressure) and are taken from tables. The Reynolds number is obtained by adding the liquid and gas Reynolds numbers, both based on superficial velocities (Groothuis & Hendal, 1959).

$$Re = Rel + Reg$$ <div style="text-align:right">Eq. 1.12</div>

Where:

Re_l… the Reynolds number of the liquid

Re_g… the Reynolds number of the gas

On the other hand, the Prandtl value is calculated only for the water (Groothuis & Hendal, 1959).

1.8 Kelvin line source theory: linear conduction model for the ground

The rock thermal conductivity (*λrock*) and the borehole thermal resistance (Rb) are determined by calculating the difference of temperatures between the secondary fluid and the undisturbed ground as a function of time, as shown in Equation 1.13. The integral in Equation 1.13 (the exponential integral) is evaluated by a series expansion referred to a work done by Ingersoll and Plass in (Acuña, Mogensen, & Palm, 2009).

$$Tbhw - Tg = \frac{q}{2 \cdot \pi \cdot L \cdot \lambda rock} \cdot \int_{\frac{rbh}{2\sqrt{\alpha t}}}^{\infty} \frac{e^{-\beta^2}}{\beta} d\beta = \frac{q}{4 \cdot \pi \cdot L \cdot \lambda rock} \cdot Ei(\frac{rb^2}{4 \cdot \alpha \cdot t})$$ <div style="text-align:right">Eq. 1.13</div>

With:

q/L… heat injection rate

α… thermal diffusivity of the ground

λ_{rock}… thermal conductivity of the rock

r_b… borehole radius

T_{bhw}…borehole wall temperature

T_g… undisturbed ground temperature

t… time since start heating

However, T_{bhw} is unknown. The temperatures experimentally obtained from the installation are T_g (taken when the ground was in undisturbed conditions), T_f and T_{gw} (taken during the experiments). To determine the resistance between the secondary fluid and the borehole wall (Rb) another term needs to be added:

Knowing:

$$Tf - Tbhw = \frac{q}{L} \cdot Rb$$ <div style="text-align:right">Eq. 1.14</div>

Then:

$$Tf - Tg = \frac{q}{L} \cdot Rb + \frac{q}{4 \cdot \pi \cdot L \cdot \lambda rock} Ei(\frac{r \cdot b^2}{4 \cdot \alpha \cdot t})$$

<div align="right">Eq. 1.15</div>

This equation is to be applied to each borehole section, that are delimited by consecutive points enumerated from F_1 to F_{26} following the flow direction, as illustrated in Figure 4. With the temperature of the fluid along the time, the R_b and λ_{rock} values can be iterated in every section until the error is acceptable.

For each section the heating power (q) is calculated with the fluid temperature difference (ΔT_s) between the water entrance and exit at every sector, and the water properties as:

$$q = \rho \cdot V \cdot Cp \cdot \Delta Ts$$

<div align="right">Eq. 1.16</div>

Where:

$\rho \ldots$ density of the water

V ... volumetric flow rate

The energy calculated in Equation 1.14 is the total energy exchanged by the sector in one way, whereas the fluid exchanges heat in both ways in every section (the way down and up). Therefore for the 12 sectors, the power value is the sum of the two power values. For instance, in section 1:

$$q1 = \rho \cdot V \cdot Cp \cdot \Delta T1.2 + \rho \cdot V \cdot Cp \cdot \Delta T25.26$$

<div align="right">Eq. 1.17</div>

The model relates the temperature of the fluid with the time, and it can be simplified. From Equation 1.13, a theoretical approximation can be used to determine the rock conductivity using the approximation:

$$Ei\frac{r2}{4 \cdot \alpha \cdot t} = \ln\left(\frac{4 \cdot \alpha \cdot t}{r^2}\right) - \gamma \qquad for \; \frac{r^2}{\alpha t} < 20$$

<div align="right">Eq. 1.18</div>

Where, in the case of $\frac{r^2}{\alpha t} = 20$, the error would be 10%, and in the case of $\frac{r^2}{\alpha t} = 5$ the error would be 2.5% (Monzó, 2011). To sum up, the dependence of the T_{bw} along the time with λ_{rock} is:

$$Tbhw - Tg = \frac{q}{4 \cdot \pi \cdot L \cdot \lambda rock} \cdot \ln(t) + \frac{q}{4 \cdot \pi \cdot L \cdot \lambda rock} \cdot \left(\ln\frac{4 \cdot \alpha}{r^2} - \gamma\right)$$

<div align="right">Eq. 1.19</div>

As said previously, the measured temperatures are from the secondary fluid and the groundwater. Therefore, with Equation 1.14, the final expression is:

$$Tf = \frac{q}{4 \cdot \pi \cdot L \cdot \lambda gw} \cdot \ln(t) + Tg + \frac{q}{4 \cdot \pi \cdot L \cdot \lambda gw} \cdot \left(\ln\frac{4 \cdot \alpha}{r^2} - \gamma\right) + \frac{q}{L} \cdot Rb$$

<div align="right">Eq. 1.20</div>

Equation 1.21 has the format of:

$$Tf = A \cdot \ln t + B \qquad A, B = constants$$

<div align="right">Eq. 1.21</div>

With A being the slope of the equation:

$$A = \frac{q}{4 \cdot \pi \cdot L \cdot \lambda rock}$$

<div align="right">Eq. 1.22</div>

The value of the slope depends on the thermal conductivity of the ground and the q/L value. With the q values calculated and a properly plotted graph, an approximation of the trend line can be determined (and thus the value of λ_{rock}).

2 Qualitative analysis of the experiments

2.1 Installation of the equipment

Figure 6: Installation of the equipment

Once the equipment was introduced, the parameters that could be modified from outside are:

- The depth of the bubble injection pipe, with a maximum value of 85 meters (the length of the pipe) into the groundwater. This modifies the value of the pressure of the N_2 needed to inject the bubbles. However, this parameter was not changed in any of the experiments carried in this thesis (with a fixed depth of the bubble injection point at 85 meters)
- The pressure of the air in the output of the tank with the pressurized valve: it allows the air to go down the pipe in a controlled way.
- The flow rate with a flow rate controller: it reduces the amount of air that can go through the pipe.
- The amount of bubbles injected with the timer: a programmable relay that blocks the output of air in a programmable sequence.

2.2 Preliminary tests

Several tests without heat injection were carried out in order to understand how the bubbles operate and to efficiently plan the DTRT.

Table 1: Preliminary tests

Test	Date	Comments
Undisturbed groundwater	19th March	No injection of bubbles
First bubble injection	20th March	Various amounts of bubbles were injected without fluid circulation.
Full bubble injection	13th April	The maximum amount of bubbles was injected, and the flow rate was calculated.

Fluid circulation with the heater OFF and full bubble injection	27th April	Transient conditions with bubbles.

2.2.1   Test 1: Analysis of the undisturbed groundwater

This test consisted on measuring the temperature of the undisturbed water for one hour (from 10:34 till 11:35). As there were two measures per minute, there were a total of 120 measurements. Figure 7 is an average profile of the temperature values along the depth during the experiment.
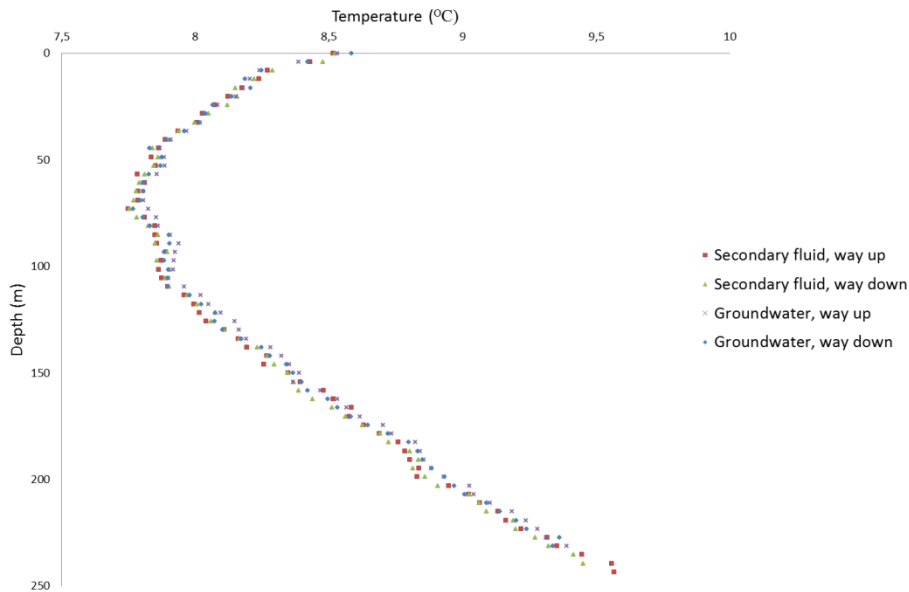
Figure 7: Temperature profile of the secondary fluid and the groundwater with undisturbed conditions

As the system had been in rest for more than a week, the equilibrium between the groundwater and the ground was considered to be reached. Therefore, this profile gives an idea of the shape of temperatures that the ground has in undisturbed conditions. Moreover, this graph has been used to properly calibrate the measurement equipment.

On the other hand, the average value of the 120 experiments is more or less precise depending on its standard deviation, which gives an idea of how far each experiment is, in average, to the average temperature of the 120 experiments. A study of the standard deviation was obtained in order to measure the precision of the measurement equipment as well as if there was any dependence between the precision of the measurement equipment with the depth of the borehole (Figure 8).
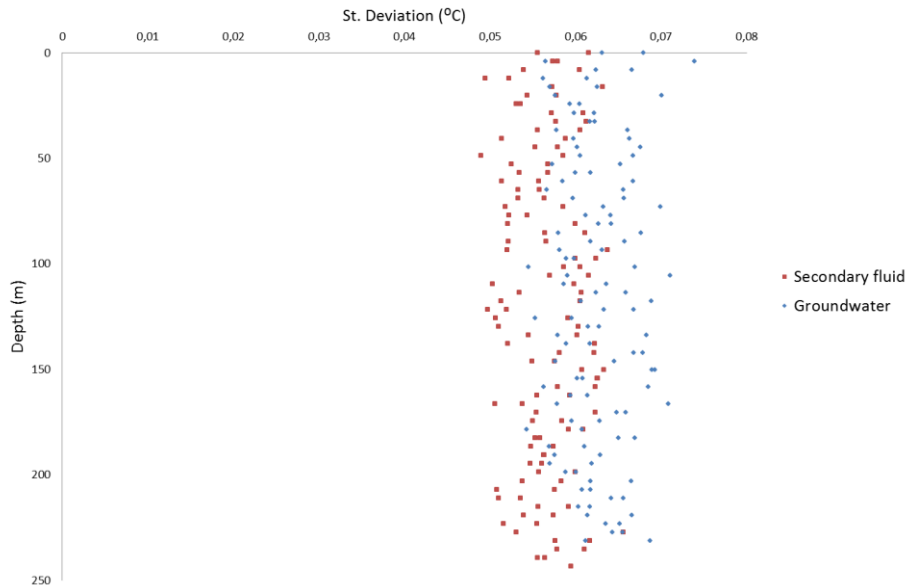
Figure 8: Standard deviation of the groundwater and secondary fluid in undisturbed conditions

The standard deviation values along the pipe range from 0.05 to 0.07 degrees, and there is no dependence of the standard deviation with the depth of the borehole, as it is shown in Figure 8. This temperature difference will be considered as the intrinsic error of the measurement equipment, meaning that there is no precision under this number. Therefore, only differences of above 0.1 degree will be considered as relevant.

2.2.2   Test 2: Analysis of bubble injection without heat injection

Starting from undisturbed conditions, there was a first study with the injection of different amount of bubbles. The flow rate controller was 50% opened, and the timer was sequenced with ON times (timer opened) and OFF times (timer closed) as follows:

Table 2: Experiments with a low rate flow of air injected

Experiment	Time	ON	OFF
2.1	11:30-11:50	5 s	2 min
2.2	11:50-12:10	5 s	1 min
2.3	12:10-12:30	5 s	30 s
2.4	12:30-12:50	5 s	20 s
2.5	12:50-13:10	5 s	10 s

The results showed very little reactions to the introduction of bubbles. Bubbles are introduced to increase the heat transfer between the borehole walls, the groundwater and the secondary fluid. One could say that by simply injecting bubbles in the groundwater without introducing heat, the equilibrium conditions are not modified, so when there is no difference of temperature there is no possible heat transfer to be enhanced. Nevertheless, some kind of reaction in the system was expected (for reasons such as the movement of water inside the borehole that may modify the profile of temperatures).

The changes seen in the graphs were of the same order as the actual standard deviation, so they cannot be used as any proof of real reaction. The most significant change in the profile was seen in the experiment number 2.5 (the one with higher air injection):
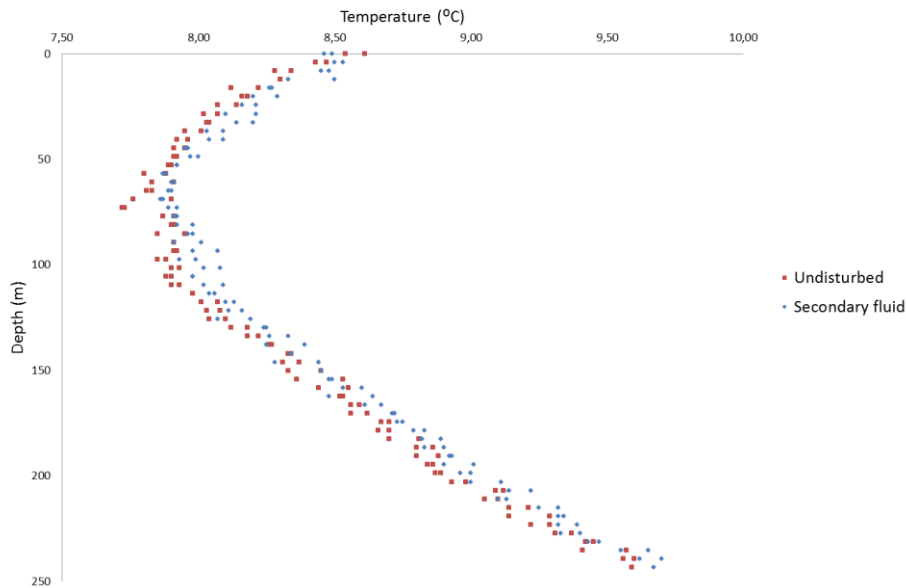
Figure 9: Temperature profile of the groundwater and the secondary fluid with bubble injection (experiment 2.5)

The conclusion at this stage was that the amount of bubbles had to be studied with more precision and also increased (as we could see no reactions at all with the first experiments with low rates, and little reactions with the last ones with higher rates). There were two ways to increase the amount of air injected: by increasing the flow rate or by increasing the injecting time. The next step is about analysing the flow rate and evaluating how it can be maximized.

2.2.3   Test 3: Maximum bubble injection

All parameters were modified in order to provide the maximum flow rate: flow controller 100% opened and maximum output pressure in the output of the tank. Once working with this flow, the total amount of bubbles would be easily controlled with the timer (allowing or not a flow of rate during a determined sequence). The air tank injected air with these conditions for 36 minutes, and the pressure of the N_2 inside the tank dropped from 98 to 96 bars. Knowing the volume of the tank (50 liters), the temperature of the air inside the tank (19.8 ºC) and using the Van der Waals equation of state with two independent variables (Equation 1.1) the mass flow rate can be calculated.

At minute 0 the pressure was 89 bars, and the calculated volume and mass are:

$$v_1 = 0.2636 \frac{l}{mol} \quad ; \quad n_1 = 189.66 \, mol$$

At minute 36 the pressure was 83 bars, and the calculated volume and mass are:

$$v_2 = 0.2829 \frac{l}{mol} \quad ; \quad n_2 = 176.76 \, mol$$

The mass difference is 12.91 mol or 361.37 grams of N_2.

In order to calculate the flow rate the Van der Waals equation must be used again taking into account the pipe conditions. In the pipe, the pressure is 9.5 bars. Considering the output of the air tank, where the temperature is also 19.5 Celsius degrees, and using the Equation 1.1 the total volume output air is $v = 2.42 \frac{l}{mol}$, and with a mass transfer of 12.91 moles the total volume is $V = 31,24$ liters. This N2 transferred in 58 minutes has a flow rate of:

$$Flow\ rate = 32.32\ \frac{l}{h}.$$

For the qualitative analysis, the undisturbed conditions were analysed first (the system had been in rest for almost two weeks). On the one hand, the standard deviation of the data obtained in these conditions was around 0.06 Celsius degrees, very similar to the values obtained in the first experiments. As before, this number is a confirmation of the margin error of the equipment, and thus differences below 0.06 will and must be neglected.

Once the undisturbed conditions were analysed, the air was injected at 16:02 without interrupting the injection with the timer. The results showed that some minutes after the air was injected the system reacted and was constantly cooled down for 10 minutes, time when the system reached the minimum temperature. The system reacted as a whole, so all the points along the depth were cooled down. Once at this temperature, the temperature globally increased for ten minutes until it reached again the undisturbed conditions, at 16:29.
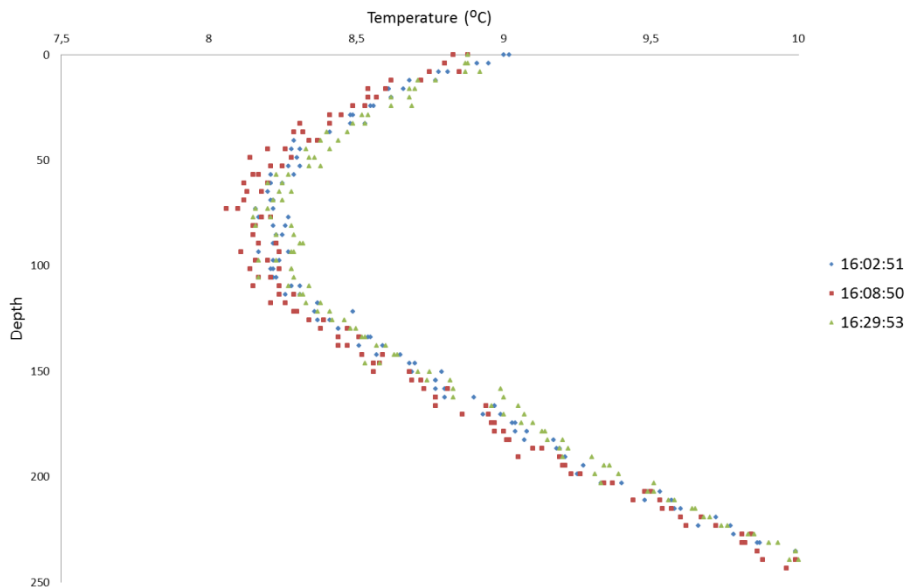
Figure 10: Comparison between temperature profiles of the groundwater in different moments of test 3

Looking at the graphs, it can be seen that the differences of temperatures in Figure 10 are higher than the standard deviation, meaning that there is enough change of temperature to ensure that the profile really changes. But the differences reached no more than 0.15 Celsius degrees.

The question to answer at this point was why the local temperature of all the measurement points of the borehole had decreased during the first ten minutes. An important point is that the system responds as a whole and all the points have their temperature decrease. There is no increasing of temperatures in any depth of the borehole, and this disables the argument that there is a transportation of water from cold to hotter areas that cools down some groundwater measurement points. If

this was the real explanation, there would be some points of the study that would be warmed up (the ones that would receive the hotter water from the hotter points).

There might be a global loss of energy in the groundwater side due to the descending of the temperatures in the groundwater. On the other hand, the borehole wall is in contact with the groundwater, but its temperature is known: the temperature profile of the borehole wall is exactly the same as the profile of the groundwater in undisturbed conditions (Figure 7).

The massive introduction of air into the groundwater creates a movement in the groundwater side that could imply an increase of the external flow of the groundwater in the bedrock. This external flow consists on the exchange of groundwater between inside and outside the borehole. The increase of water coming from the cracks could provide water with a lower temperature than the temperature of the borehole wall. However, the borehole had rested until undisturbed conditions were achieved before these experiments were done, so the slight decrease and increase in temperature might have to do with the accuracy of the measurement instrument itself. If this is not the case, the forced convection between the groundwater and the walls (enhanced by the bubbles) might help in bringing the system back to the original temperature. On the other hand, the temperature change of the instrument while start up may be affecting these conclusions.

On the other hand, the influence of the heat transfer in terms of the position in the borehole has also been evaluated. A conclusion for this test may be that the consequences of injecting bubbles at a depth of 85 meters affect all the borehole length in a similar way. In Figure 11 it can be seen that the changes of temperatures in the moment of bubble injection obey the same patterns:
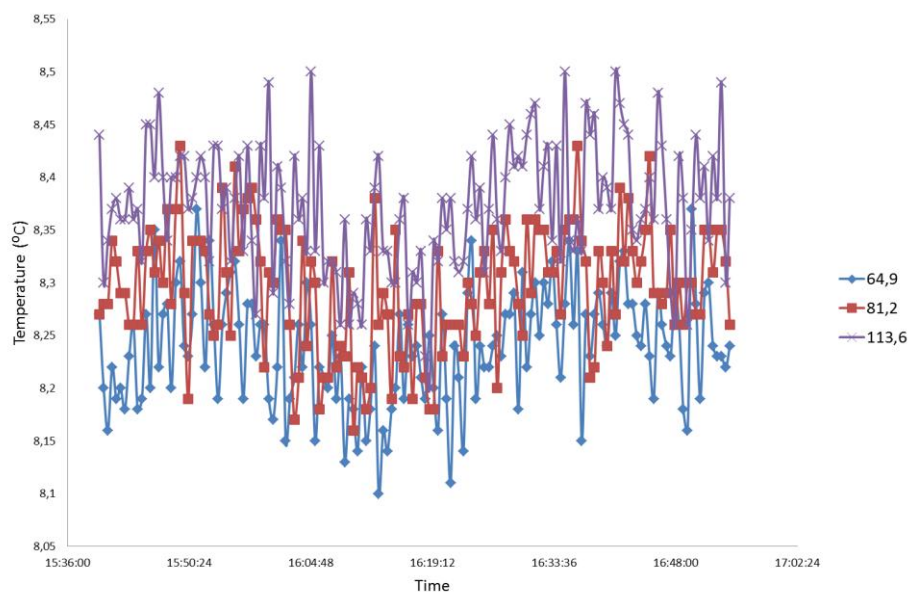
Figure 11: Comparison of the temperature profiles of the groundwater at different depths

2.2.4   Test 4: Fluid circulation without heating

The pump that activates the circulation of the secondary fluid was turned on at 15:01 the 27th of April, and the secondary fluid started to flow without bubble injection in the groundwater side. The temperature along the borehole of the secondary fluid evolved to the equilibrium. The equilibrium is, in this case, the average temperature of the groundwater side, or in other words, the average of all measurement points before the flow started. In the beginning, the transient conditions lasted for 25 minutes and then the profile started to stabilize.
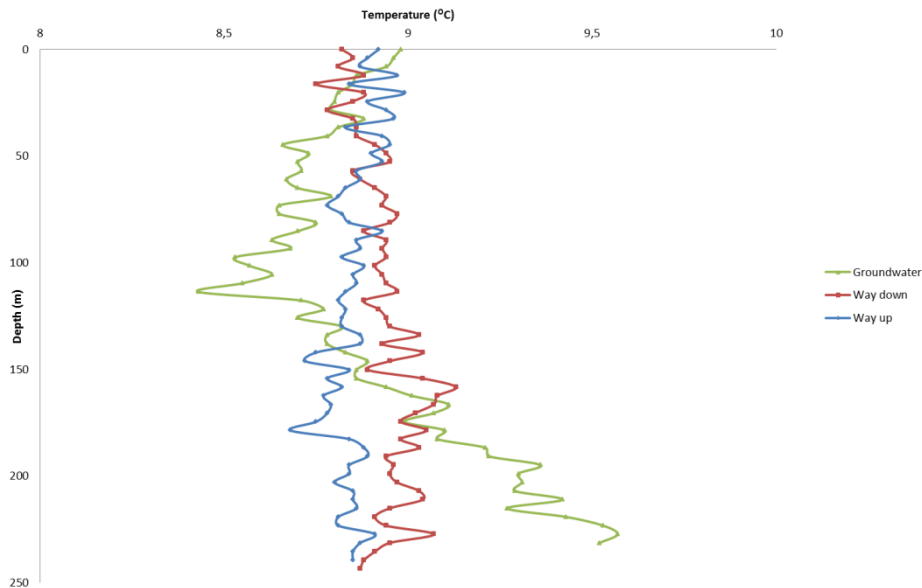
Figure 12: Temperature profile of the groundwater and the secondary fluid

At 16:00, the bubbles were injected with the maximum flow rate. No relevant changes occurred to the profile.

2.2.5   Calculation of the velocity of the bubbles. Video recording

A video camera was introduced inside the borehole to capture images and videos of all the equipment, pipes, structures and surroundings. The video camera consisted in a small device with a diameter of 4 centimeters and a length of 15 centimeters. It was held by a hose that allowed to introduce the camera in a depth of 200 meters. The small dimensions of the whole video equipment were necessary to take images in such a small space with already a lot of pipes and cables.

The first videos recorded the input of pipes inside the borehole, the very first meters of the borehole, covered by steel, and finally the rock and the groundwater. Images of the undisturbed conditions as well as clear pictures of the pipes and the measurement equipment were taken.

Secondly, the bubble injector was activated. The video recorded the bubbles coming from the depths and showed a very active motion of the bubbles. The flow of the bubbles was constant, with constantly a video scene full of bubbles, and the size of the bubbles was also estimated to be from some millimeters till 1 or 2 centimeters of bubble diameter. In the videos one can also see that there were a lot of particles moving around. These particles came from the rock because they were removed by the movement of bubbles inside the groundwater.

There were images taken from different depths: from above the groundwater level, from some centimeters below the groundwater level and from a depth of 16.5 meters. In all of them, the bubbles had a similar aspect, although they seemed to be bigger in shorter depths. This phenomenon is due to the lower pressure in the water at lower depths.

Furthermore, one of the main objectives of the recording was to calculate the velocity of the bubbles. The bubbles are injected at a depth of approximately 85 meters below the groundwater level. When they are injected, they are pushed upwards until they reach the groundwater level. When studying the dynamics, there are mainly three forces pushing the bubbles. The first one is the weight of the bubble itself, with its direction going downwards towards the kernel of the Earth. The

second force is the Arquimedes force, that consists on a force that is equal to the weight of the water displaced by the bubble, with an onwards direction. The last force is the friction force with its direction against the movement of the bubble. The balance of the two former forces determines the direction of the movement, and the friction pushes against this movement. The equivalent force generates an acceleration of the bubble.

In the case of the air bubbles inside the groundwater, the Arquimedes force is higher than the weight of the bubble (a volume of water is heavier than the same volume of air). When the bubbles are injected at 85meters depth, as the equivalent force goes onwards there is an acceleration of the bubble in this direction. However, the friction with the water depends on the speed of bubble (the faster the bubble goes, the higher the friction force is). When the bubble is accelerating, it speeds up and the friction force arises until it eventually reaches the value of the equivalent force onwards. At this point, the forces are balanced and the acceleration is eliminated: the bubble has a constant speed.

In order to experimentally calculate what the exact speed of the bubbles was, the camera was first located in the groundwater level. The time between the bubble injector was activated and the bubbles appeared on the surface was 4 minutes and 15 seconds. Then, a second experiment was done: measurement of the time between the bubble injector being stopped and the last bubble to arrive to the surface: it took 4 minutes for the last bubble to go from the injector to the groundwater level. One reason that can explain the difference of 15 seconds is the activation time of the Booster that consists on the time that it takes for the air tank to push the remaining water in the bubble pipe until it actually starts injecting bubbles. For this reason, the second experiment is considered to be more accurate for the calculation of the bubble speed through the groundwater. A third experiment was done in a deeper location, at 16.5 meters below the groundwater level. The time between the injector being stopped and the last bubbles was 3 minutes and 30 seconds.

Table 3: Results of the average speed of the bubbles at different depths

Distance covered by the bubbles	Time taken	Average speed
85 meters	4 minutes	21.25 m/min
68,5 meters	3 minutes 30 seconds	19.57 m/min

In the last 16.5 meters, the bubbles have a higher speed than the first 68.5 meters, corresponding to the theory explained above the table: the bubbles start at a speed of 0 where they are injected in a depth of 85 meters, and gain velocity until they reach the dynamic equilibrium.

It is clear that in the first 68.5 meters the process of accelerating lowers down the average speed, but it is not sure that the last 16.5 m. the forces are completely balanced and therefore the speed is constant. However, with the values obtained the average speed of the last 16.5 meters is 33 m/min.

2.3   Distributed Thermal Response Test

A DTRT divided in five phases is the main experiment of this thesis. In all phases the heater was activated (9 kW) and the fluid circulated at a flow of 1.6 m^3/h.

Table 4: DTRT with the two bubble phases

	Heat injection	Experiment 1: Full Bubble injection	Recovery with no bubbles	Experiment 2: Half bubble injection	Recovery with no bubbles
Date	April 30th	May 4th	May 5th	May 9th	May 10th
Starting Time	14:48	17:07	16:10	15:24	14.00
Condition	No bubbles	Full bubbles	No bubbles	Half bubbles	No bubbles

2.4 Experiment 1: Injection of bubbles at the maximum rate

This experiment is a continuation of the preliminary test 4, when the fluid started to circulate in heating conditions and with full bubble injection. Before injecting bubbles the secondary fluid had reached the stationary conditions (better known as stead-flux), as defined by the Equation 1.18. In the moment of bubbling this condition had the value of 0.0018.

At this time, reached the steady flux conditions, the temperature profile had the same shape along the time although the trend of the system was to move to higher temperatures. This trend can be explained with the energy that is constantly given to the system (when the heater is on). This energy is introduced into the system and absorbed by the groundwater, the pipes, the borehole wall and the ground, which are later heated up. So, even though the profile is considered to be in stationary conditions, the profile moves uniformly to higher temperatures.

In this experiment, with the heater on and with bubble injection, on May 4th at 17:07 the injector timer was connected allowing the air flow from the tank through the pipes. The air inside the pipe needs a pressure of 8.5 bars in order to be able to get into the groundwater, and initially there was no air inside the pipes. Three minutes were needed to pressurize the pipes with air before the air could actually get inside the groundwater. At 17.10 the manometer registered a pressure inside the pipe of 8.5 bars, time when the air started to escape in a bubble form inside the groundwater.

2.4.1 Analysis of the temperature profile along the depth

In Figure 13, the first half an hour of bubbling is studied. There are mainly four changes in the temperature profile:
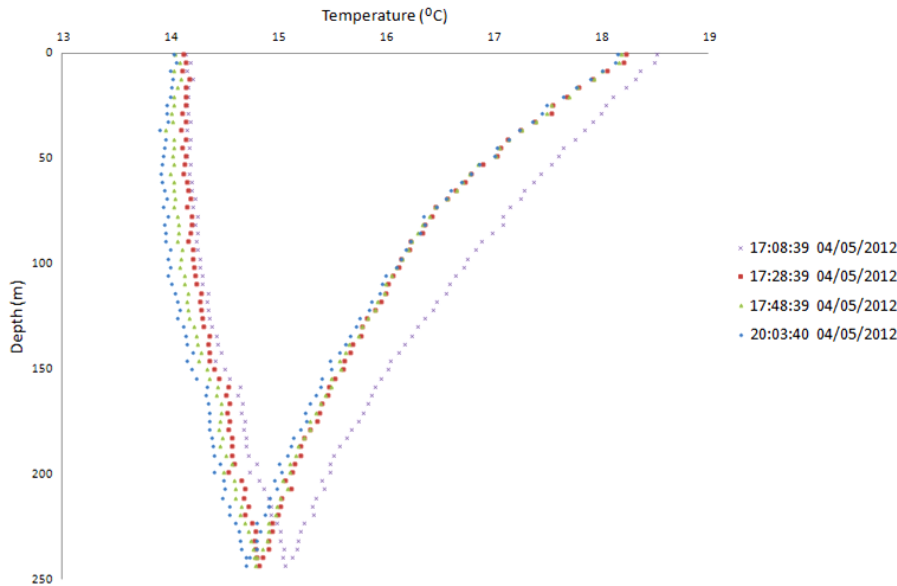
Figure 13: Change in the profile of the secondary fluid in the first half an hour of bubble injection (Experiment 1)

The purple profile (17:08) shows the steady flux condition in heating mode just before the bubble injection. It shows that the exchange of energy is mainly done in the downward direction of the pipe: the secondary fluid that comes from the pump gets inside the borehole at a temperature of about 18.25 Celsius degrees. It provides energy to the ground along the borehole until the temperature is around 15 Celsius degrees at the bottom of the borehole. . Then, it is heated about one degree in the upwards direction. The heat transferred downwards represents the about 80% of the total.

At 17:10 the bubbles started to flow into the groundwater, and only eighteen minutes after (red profile) there are already substantial changes in the profile. The temperatures in the downwards direction are clearly reduced. There is also a reduction of the output and input fluid temperatures, although the difference between them is constant (in fact, this difference is only function of the energy injected by the heater and the flow of fluid, which is maintained). The temperature in the bottom is lowers down around 0.3 degrees, implying that at this stage a bigger percentage of the heat transfer is done on the way down (85 % of the total), suggesting that the bubble injection allows a bigger absorption of energy in the downwards direction. Finally, the part affected at 17:28 is only the way down the pipe (where the heat transfer is actually mainly taking place).

Twenty minutes later, at 17:48, around half an hour after injecting bubbles, the profile doesn't show significant changes in the way down. However, on the upwards direction the profile has some small changes: the temperatures are slightly lowered down along the borehole.

Finally, after analysing the trend of the temperature profiles along the time, small changes occur in the profile until it is stabilized at 20:03. From that moment and until the end of experiment 1, the profile moves uniformly to the right, as it can be seen in Figure 14. As explained previously, the system is slowly heated up due to the fact that energy is introduced to the system. The input and output temperatures are increased, and the whole profile is warmed up.
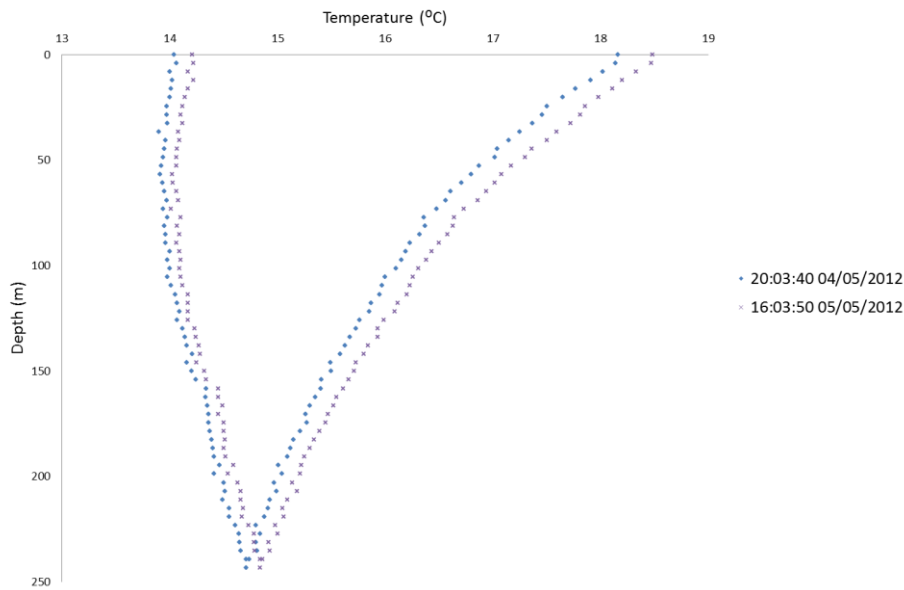
Figure 14: Change of the profile in the secondary fluid in stationary conditions while injecting bubbles

The groundwater temperature profile also shows more significant results. First of all, it shows a more inertial behaviour compared to the secondary fluid, because it has taken longer time to detect important changes in the profile. After 30 minutes of bubble injection, at 17:38, the groundwater showed the first changes, as it is shown in Figure 14.
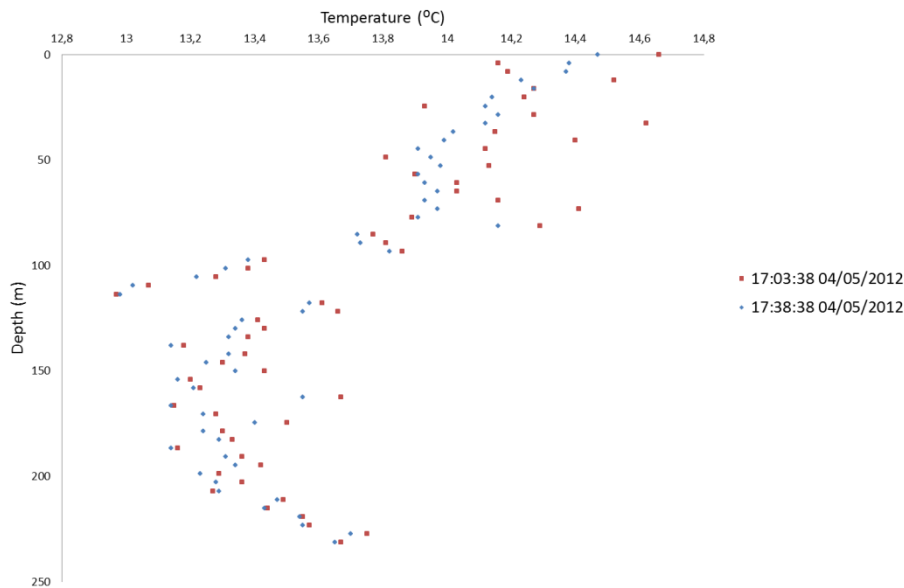
Figure 15: Groundwater temperature profile comparison between before and after 30 minutes of injecting bubbles

A homogenization of the temperatures in the upper part of the borehole (above the injection point) can be observed. This homogenization implies that the temperatures in every measurement point are less dispersed from each other and more ordered. The fact that they are more ordered implies a reduction of the insulation effect of the groundwater. To sum up, the homogenization indicates a reduction of the thermal resistance between the groundwater and the borehole wall.

Under the injection point, a minimal reduction of temperatures of the measurement points is detected (at a similar level to the standard deviation of the data obtained in undisturbed conditions

with the equipment). Moreover, under the injection point the groundwater does not homogenise the temperature of the measurement points.
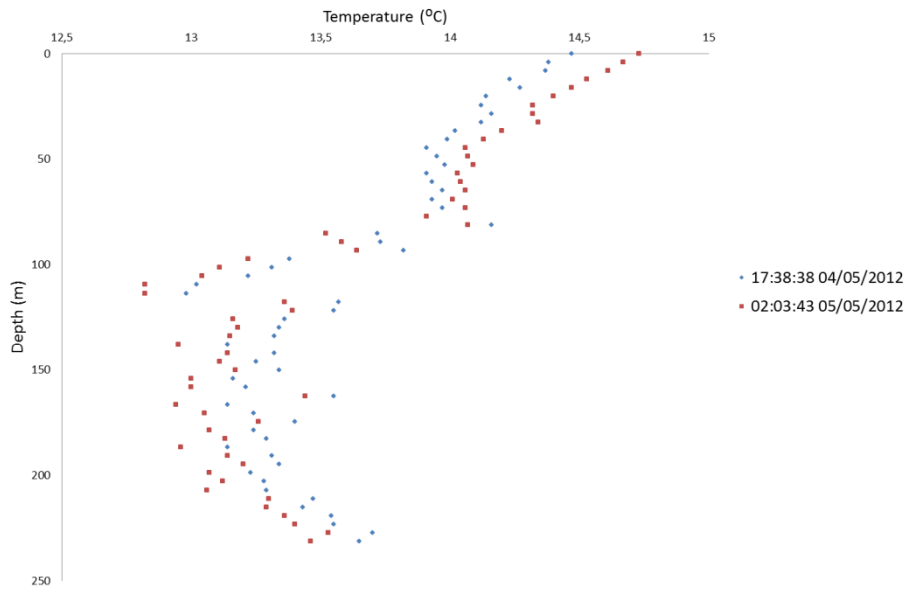
Figure 16: Evolution of the temperature profile of the groundwater in stationary conditions

The system reaches somewhat stationary conditions the day after at 2:03 (Figure 16). From this point, the profile does not change in shape, although it keeps slowly increasing its temperature because once the stationary conditions are achieved, the only change the system does is to globally warm up (Figure 17).
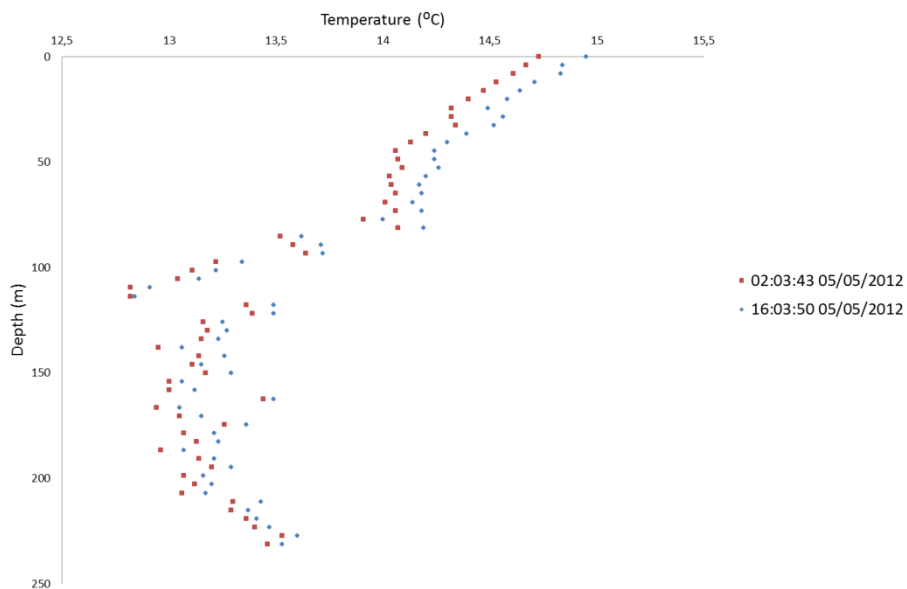
Figure 17: Temperature profile of the groundwater in stationary conditions

Furthermore, the measurement equipment measures twice the temperature every four meters in the groundwater side. The study of the data showed that there was no difference at all between the two measures.

After all, what is important is the relation between the temperatures of the secondary fluid and the groundwater. The difference between them allows the heat transfer and determines how the convection is enhanced depending on the distance between them in the profiles, whether is shortened or not.

In the beginning, with the heater on and without bubbles, both profiles show the shape in Figure 18:
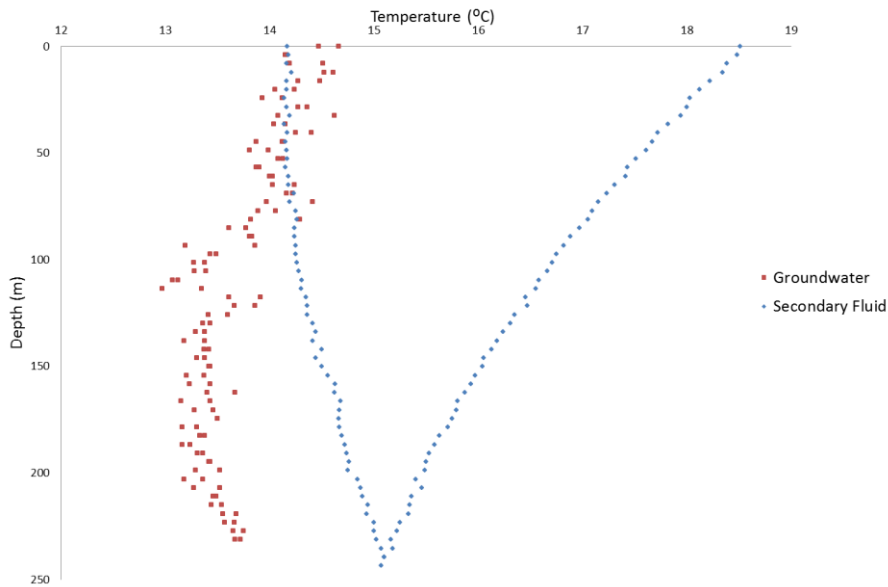
Figure 18: Secondary fluid and groundwater profiles before injecting bubbles (at 17:00)

Half an hour after starting the bubble injection, both profiles get closer as shown in Figure 19:
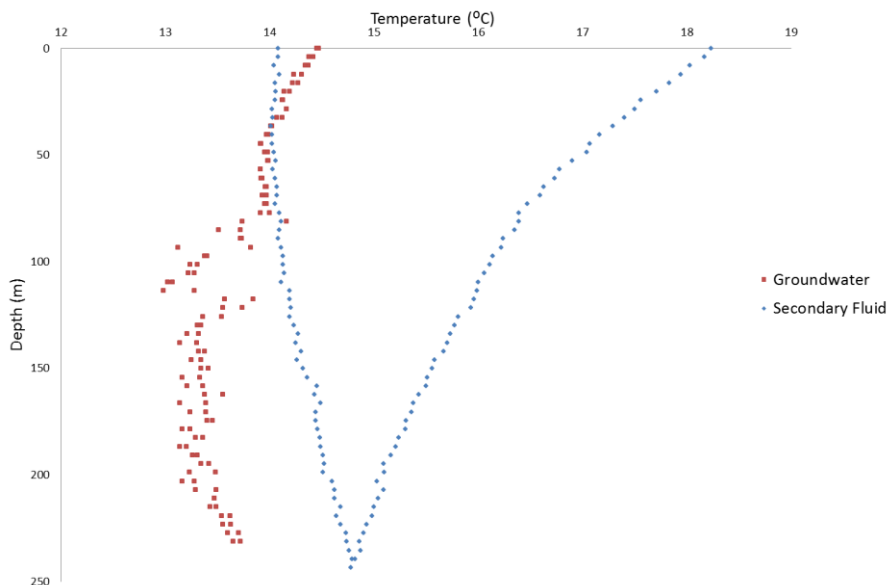
Figure 19: Secondary fluid and groundwater profiles half an hour after bubble injection (17:38)

The first change is that the shape of both profiles looks more alike with bubbles than without, with a higher degree of parallelism, which is due to the better heat transfer between the groundwater and the secondary fluid.

At 2.03 the day after, the groundwater side reaches the stationary conditions. It is clear that the convection between the fluid and the groundwater is enhanced, because the two different substances that initially have different temperatures (secondary fluid and groundwater) tend to equal their temperatures (Figure 20).
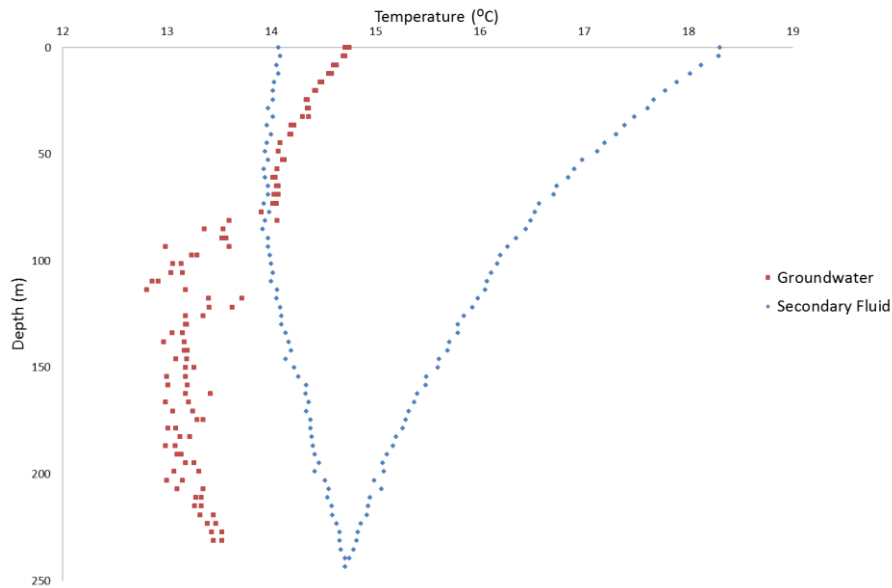
Figure 20: Secondary fluid and groundwater profiles in stationary conditions with bubble injection (2:03)

The shape of the profiles (shown in Figure 20) of the groundwater side and the secondary fluid on the way down are identical. Also, on the way up of the secondary fluid, the difference of temperatures with the groundwater is negligible in the upper parts or even negative above the 75 meters of depth. Due to the usage of the bubbles, the heat transfer on the way up of the borehole is negligible. This feature is something that the work of (Acuña J. , 2010) has always tried to avoid: the symmetry of the profile is a sign of a better efficiency in the heat exchanger. A conclusion from this apparent contradiction is that the long depth of the borehole is not needed. With a shorter borehole the same objective seemed that could be achieved. In the case of a 100 meters borehole, for example, a correct symmetry could presumably be achieved. However, a shorter borehole implies a smaller sink to transfer heat to, and that may have bad consequences in the long term efficiency of the borehole.

2.4.2   Analysis of the temperature profile along the time

When analysing the same data in terms of location instead of time, it can be clearly seen when each measurement point reaches the stationary conditions and what differences the temperature profile suffers depending on the depth. Figure 21 shows how the profile is changed with the bubble injection at a low depth (56.8 m):

Figure 21: Temperature profile of the secondary fluid at a depth of 56.8 meters (way down)

The reaction time is very short, and at 17:43 the system stabilise at 0.13 Celsius degrees lower. Then, the secondary fluid is slowly he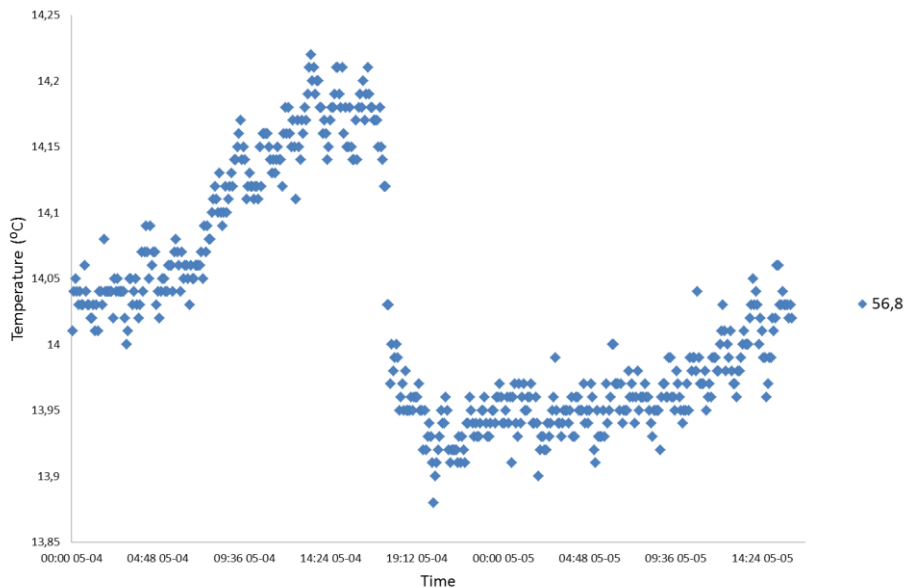ated up until the end of the experiment, due to the external heat injection. At the end of the experiment, around 23 hours after starting the injection of bubbles, the temperature reaches the initial 14.15 degrees.

However, this particular profile differs depending on the depth. To evaluate the differences along the depth, the parameters that have been studied are the initial temperature, the variation of temperature due to the bubble effect until it reaches stationary conditions and the temperature at the end of the experiment.

The reduction of the thermal resistance is evaluated with the difference of temperatures between the initial temperature and the one of the stationary conditions, because the only reason why the temperature decreases is that the convection is enhanced. The consequence of the bubbles is to increase the convection heat transfer coefficient and reduce the groundwater insulation effect, which is why there is a sudden drop. Thus, this parameter helps understanding what is going on with the convection at that point. The ΔT increases its value along the borehole. This means that the heat transfer is enhanced above and below the injection point, even though the bubbles only travel inside the groundwater above the injection point.

The final temperature gives an idea of how fast the reheat has taken place. It happens along the borehole that the slope of the temperature as a function of time seems to be lower with bubbles than without bubbles.

In the case of analyzing the temperature profile of the groundwater in a fixed depth along the time, two sectors are distinguished: above the bubble injection point and below of it. The parameters studied in this analysis are the initial drop of temperature, the recovery of the drop and the reheating slope.

Above the injection point, the temperature profile shows a sudden drop of its temperature of around 0.2 Celsius degrees at the moment of starting the bubble injection. In the first 30 meters, the measurement points recover the drop of temperatures approximately two hours after the bubble injection started, where they reach the temperature they would have had if no bubbles were in-

jected (on the trend line of the temperature before injecting bubbles, Figure 22. After that, the slope of the temperature graph is maintained slightly lower in relation to the slope previous to the bubble injection (the numeric values of the change of slope will be seen in the quantitative analysis). At this depth, the secondary fluid decreases more its temperature with bubbles than without bubbles.
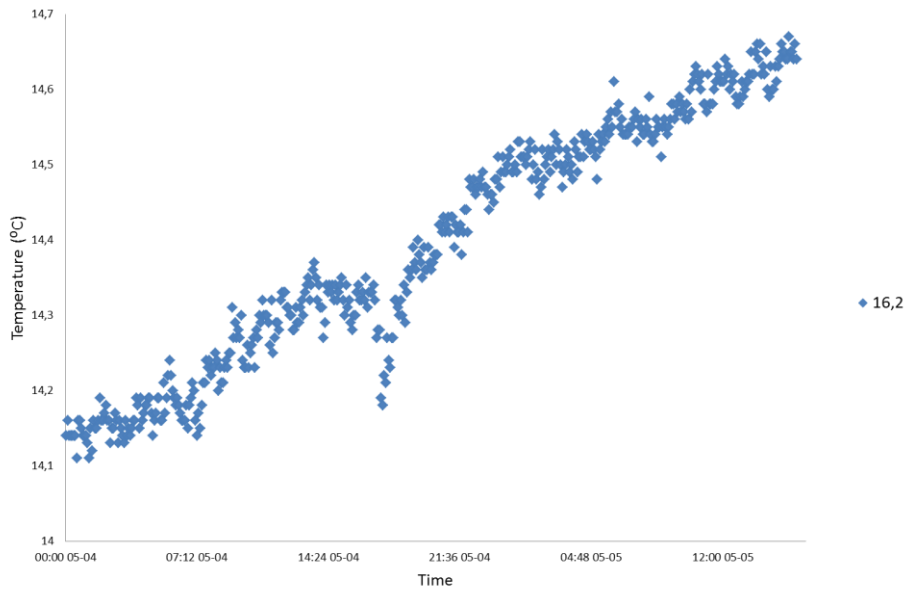
Figure 22: Groundwater temperature profile at a depth of 16.2 meters

Between meter 30 until the injection point (at around 85 meters depth), the pattern is slightly different (Figure 23). There is not a complete recovery after the initial sudden drop of temperature, which is also around 0.2 degrees. Instead of a total recovery, it is partial and completed at around 20:30, where the temperature is lower than the expected temperature if the bubbles would not have been injected (that is, if a trend line is calculated from the data previous to the bubble injection). Secondly, the slope of the temperature profile is changed after the partial recovery and compared to the slope previous to the injection. The trend is that the slope decreases somewhat, indicating the enhancement in heat transfer. On the other hand, at these depths the reduction of the temperature in the secondary fluid is higher with bubbles.
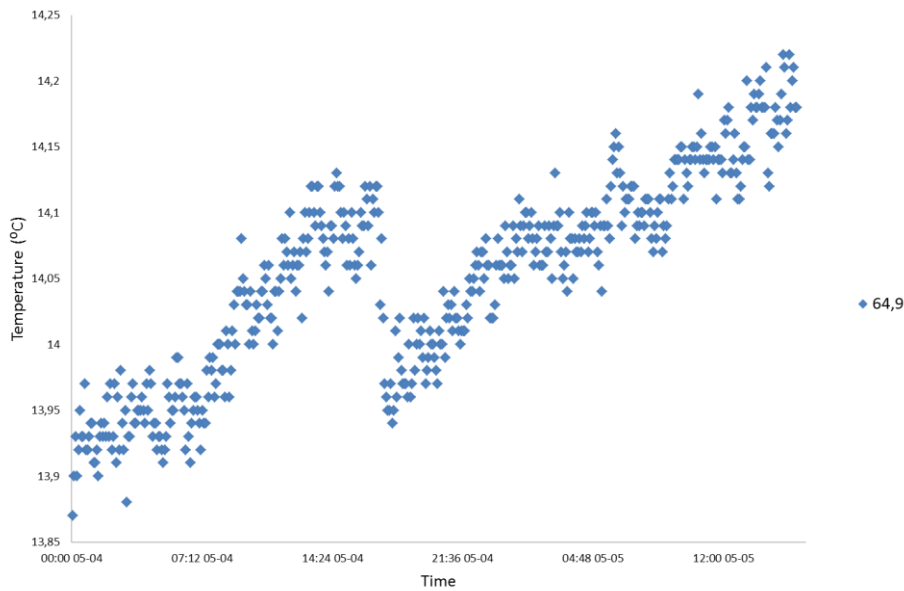
Figure 23: Groundwater temperature profile at a depth of 64.9 meters

However, below the injection point higher changes are detected (Figure 24). To start with, the drop of temperature is even higher than in points above the injection point, around 0.3 degrees. The second important change is that there is no recovery of the initial drop, not even partially. The third important change is about the slope, which clearly decreases.
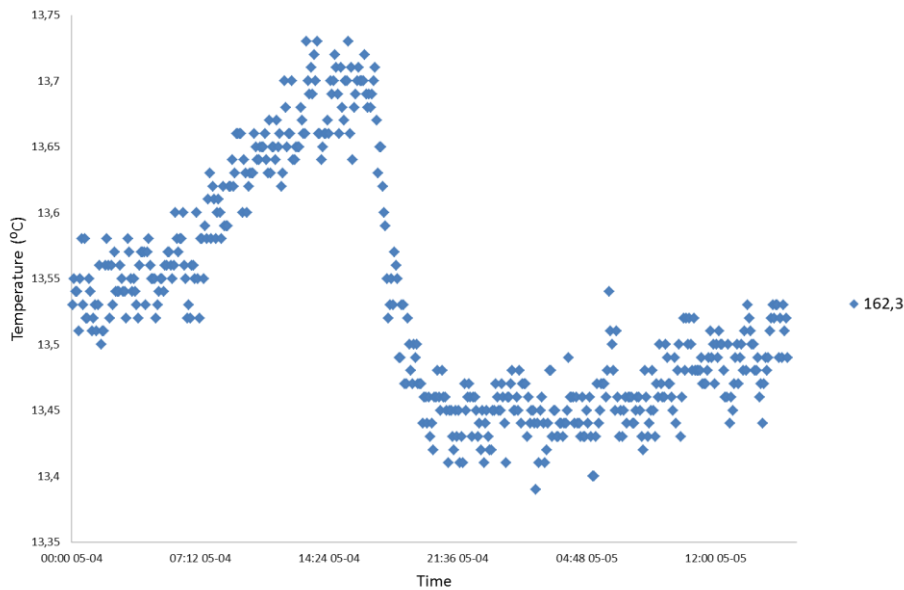
Figure 24: Groundwater temperature profile at a depth of 162.3 meters

The overall point in the groundwater is that it suddenly lowers its temperature (reducing the thermal resistance with the borehole walls) and it reduces the slope of the temperature along the time (transferring the heat forward to the rock). Moreover, it seems that the heat transfer in the rock is not only enhanced along the borehole, but even more in lower parts of the injection point, especially at deeper parts where the drop is higher and unrecovered. However, the resistance between the borehole wall and the secondary fluid is reduced in the upper part. These two facts combined might conclude that the improvement is done equally along the borehole.

2.5 Experiment 2: Injection of bubbles at the middle flow rate

After the maximum bubble injection, the system was left in heating conditions without bubbles for four days in a non-bubble recovery process.

The second experiment, carried on May 9th, consisted on injecting a lower rate of bubbles to analyze if the amount of bubbles could be optimized in relation to the enhancement of the efficiency. Before starting the experiment, at 14:16, it was noticed that the flow rate was lower than in the first experiment. A couple of liters of water were introduced in the secondary pipes and the regulation valves were adjusted. However, the injection of water (which was colder than the average temperature of the secondary fluid) had its effects on the temperature profile of the secondary fluid along the borehole.

The system was left in rest for one hour to reach the stationary conditions. After 1 hour the system had reached a constant profile shape. At 15:27, the air tank was oppened with a different timer sequence: 3 minutes ON, 3 minutes OFF. The objective of this sequence was to provide half of the maximum flow while ensuring that there constantly were bubbles in some parts of the borehole. As it takes 4 minutes for the bubbles to reach the surface, 3 minutes is a shorter time that allows the constant presence of bubbles in the borehole as well as minimizes the possible peak of air injected every time that the timer changes form ON to OFF. The exact amount of air spent during the experiment can be determined with the difference of pressure in the tank caused by the injection of bubbles. The pressure in the air tank before the experiment was 81 bar, until it lowered to 8.5 bars at the end of experiment. Knowing the volume (50 liters) and the initial and final temperatures (21.3 and 21.6 Celsius degrees), the nitrogen mass can be calculated with the Van der Waals equation (Equation 1.1):

$$\Delta n = 151{,}88 \; mol \qquad Flow \; rate = 17{,}23 \; l/h$$

And in comparison with the mass spent in the first experiment. It represents a reduction of 46.7% of the bubbles spent in the first experiment.

2.5.1 Analysis of the temperature profile along the depth

In the first half an hour of the second experiment, the qualitative changes in the fluid temperature profile are similar to the ones with maximum bubble injection, although the differences in absolute numbers are slightly lower. Moreover, the reaction time of the process is similar to the other experiment, around half an hour until the systems seem to have a stationary profile shape. Figure 25 compares the effect of the first three hours in both experiments on the secondary fluid side: on the left, the two profiles are from the experiment with maximum bubbles (also in Figure 12) and the two profiles on the right are done with the half bubble rate.
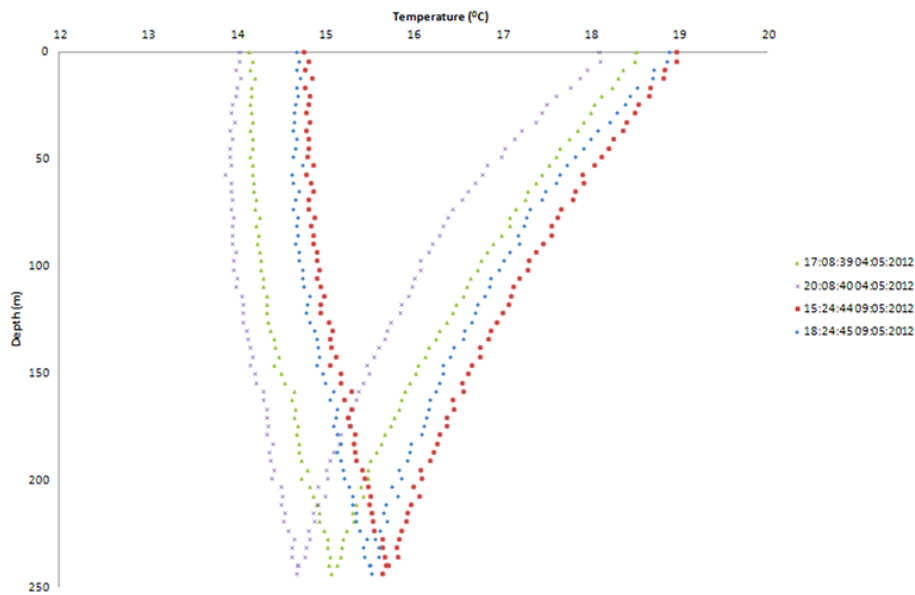
Figure 25: Change in the profile of the secondary fluid in the first half an hour of bubble injection

The changes are more abrupt in the first experiment (with more difference of temperatures). The slope on the way down is more pronounced; the heat transfer is done in higher depths in the first experiment. Comparing these two cases with the profile without bubbles, there is a relation of transferring the heat in lower depths and the amount of bubbles.

On the other hand, after the initial drop the system starts to warm up, identically to the case with full bubble injection.

In the case of the injection of half bubbles, the signs that affect the profiles are identical to the full bubble signs, but in a lower scale. There is a lower homogenization, and a lower decreasing of temperatures. However, once the stationary conditions are achieved, the system globally heats up in a similar way.

With both the secondary fluid and groundwater profiles combined, these differences can be also appreciated.

Figure 26: Secondary fluid and groundwater profiles in stationary conditions with bubble injection (22:00)

Compared to the same Figure in the experiment 1 (Figure 20), the three main differences in the second experiment are:

- The lower homogenization of the profile, especially detectable above the injection point.
- The less abrupt slope in the downwards direction in both the secondary fluid side and in the groundwater side.
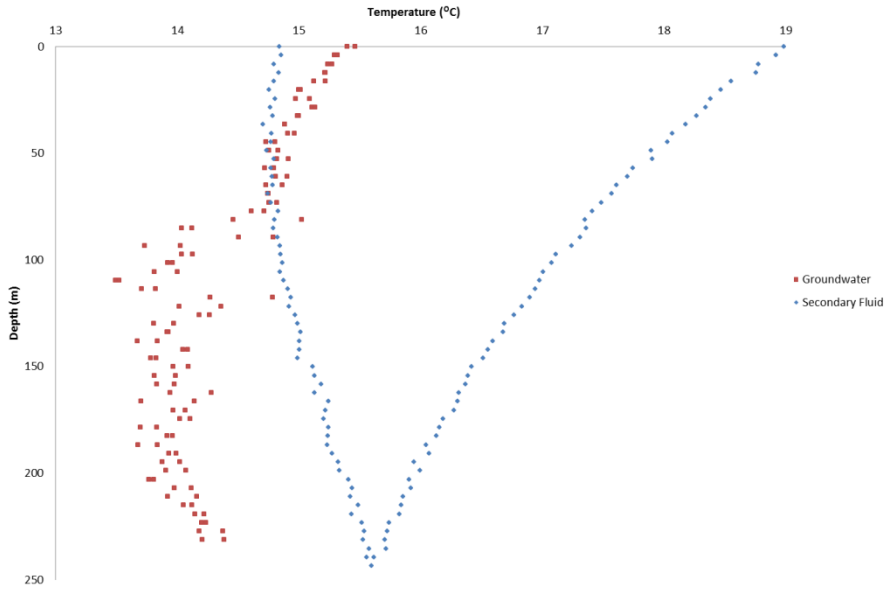- The lower approximation between the two profiles and the higher difference between the secondary fluid and the groundwater side.

2.5.2   Analysis of the temperature profile along the time

Furthermore, the study of every measurement point along the time also shows other differences between the two cases. Qualitatively, the changes in the shape of the profiles are very similar to the full bubble experiment, which supports the conclusions reported in the previous chapter in terms of changes in shape.

One change compared to the previous experiment is the value of the initial temperature drops in the secondary fluid caused by the bubbles. First of all, the drops are less abrupt in the case of half-bubble injection. In the first 100 meters of depth in the downwards direction, the drop of temperatures is similar in both experiments, around 0.2 degrees. Below 100 meters, the drop of temperature in the first experiment is twice the one in the second experiment, and below 200 meters the drop is between two and three times bigger in the first experiment.

In terms of the time taken by the system to stabilize the temperature and start reheating, it takes similar times in both experiments. There is no relation between the time taken to recover and the bubble injection.

When comparing the temperature profiles of the groundwater side in the two experiments, the Equation 1.20 has been taken into account. The slope of the temperature profile is logarithmic with the time origin in the start of the heat injection. Therefore, the slope of the logarithm depends on

the time apart from the rock conductivity. This model is based on pure heat conduction in the ground, which may not be the case in these experiments, so this analysis only attempts to estimate and roughly quantify what happens in the surrounding ground while injecting bubbles.

When comparing the slopes, the difference of slope between after and before the bubble injection for each experiment is considered. In the case of a low depth (Figure 27) there is a bigger drop of temperature, and the reduction is hardly noticeable.

In Figures 27, 28 and 29, the slope comparison is qualitatively presented at different depths. The main horizontal axis is related to the time for the second experiment and the secondary horizontal axis to the first experiment.
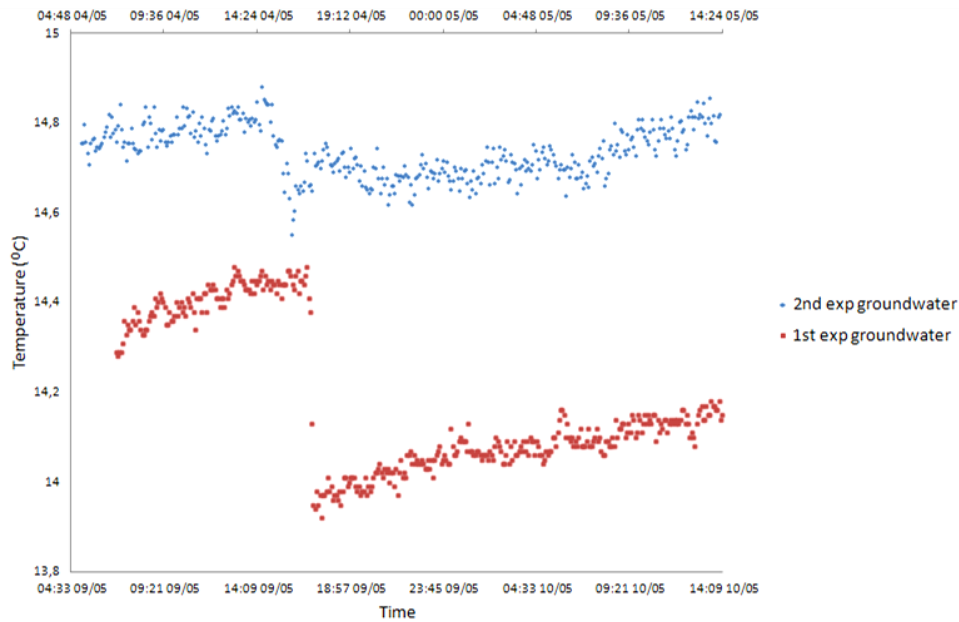
Figure 27 Comparison of the groundwater temperature profiles at a depth of 73 meters

The differences are increased at larger depths, like in Figure 28, where not only a big difference in the magnitude of the temperature drop can be seen, but also the difference of slopes is clear while full bubble injection. On the other hand, it can also be appreciated that there is a bigger homogenization of the temperatures in the first experiment.
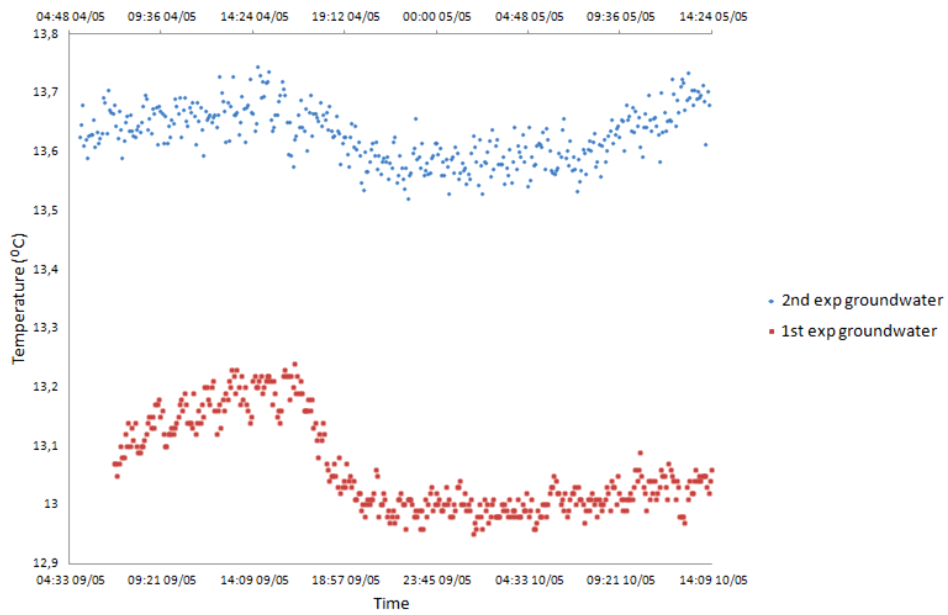
Figure 28: Comparison of the groundwater temperature profiles at a depth of 186.7 meters

In deeper points, the difference in the slopes and in the initial drop increases (Figure 29).
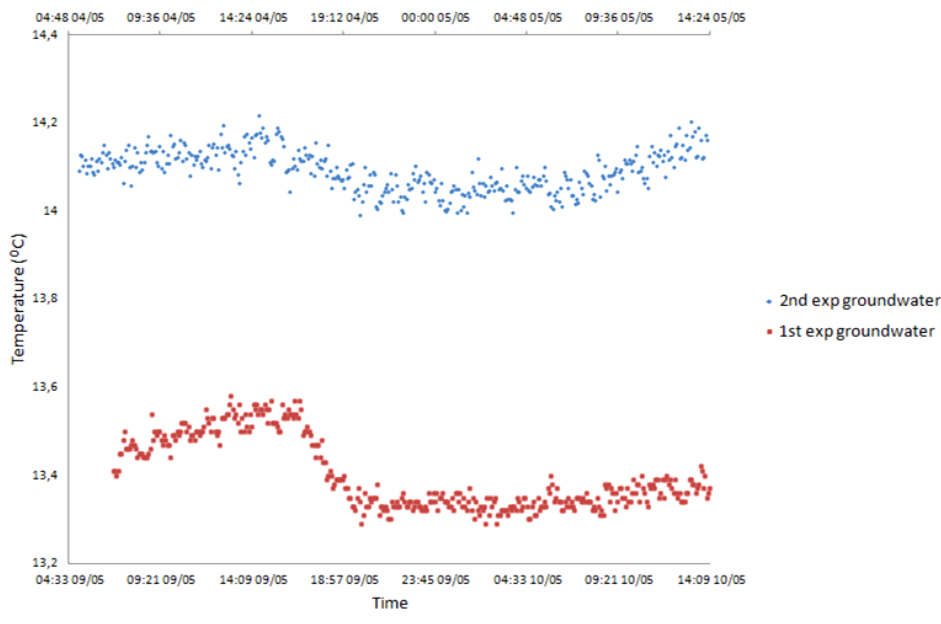

Figure 29: Comparison of the groundwater temperature profiles at a depth of 211 meters

This change of slope clearly indicates that the heat coming from the heater is rather transferred to the ground than kept by the groundwater when more bubbles are injected.

2.5 Analysis of the recovery process. Heat injection without bubbles

When the bubble injector was turned off the recovery process revealed that the effect of the bubbles is reciprocal. It is very interesting to analyse the whole experiment (table 4) in a single graph (Figure 30), since heat is injected along the time.
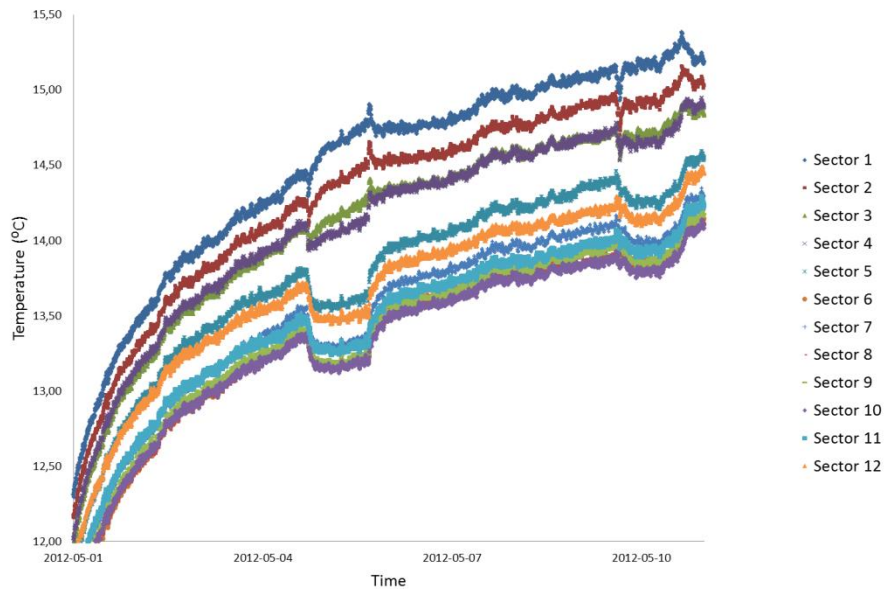
Figure 30: Temperature profile of the groundwater during the DTRT

Once the bubbles are not injected the borehole rapidly recuperates the logarithmic profile that both the secondary fluid and the groundwater had before the bubble injection. It can be seen in Figure 30 that the profile of the system is only temporally disturbed in the moment of bubble injection. When the bubble injector is turned off the temperature profile returns to the position that it would have had if no bubbles had been previously injected. However, not only there is a complete recuperation of the temperature, but it is also done at a high speed, similarly to the change when the bubbles are first injected. First, there is a sudden temperature rise whose value is similar to the previous temperature drop. Then, the slope of the temperature profile is also increased. The capacity of the system to transfer the heat to the rock is reduced.

On the other hand, the temperature profiles of the secondary fluid and the groundwater act as a whole system, as they follow the same profile patterns although their temperatures are 2 Celsius degrees different (Figure 31). This difference represents the thermal resistance between them, and it can be appreciated that the difference is smaller when there are bubbles.
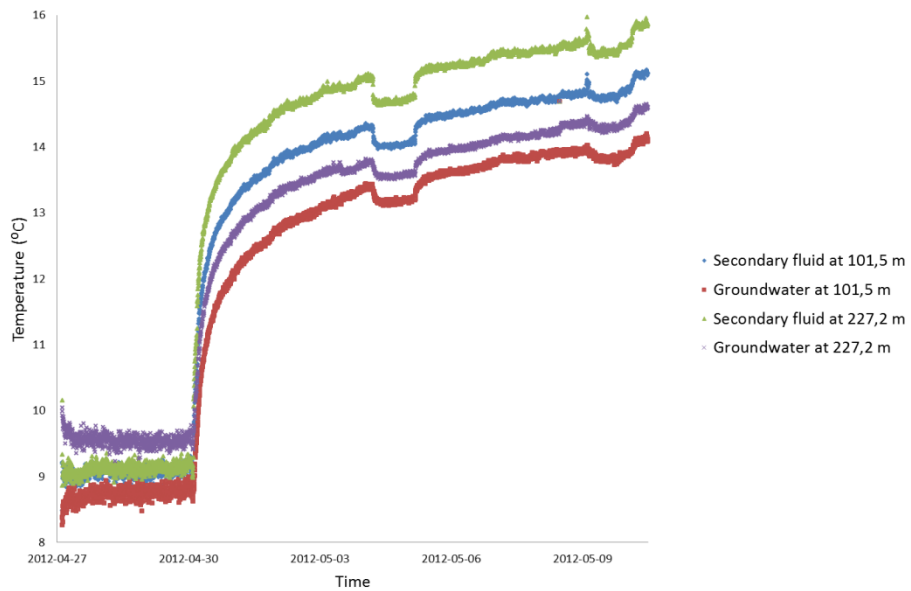
Figure 31: Temperature profile of the groundwater and the secondary fluid during the DTRT

The effect of stopping the bubble injection is like the effect of insulating the fluid from the groundwater. The bubble injection helps transferring the energy more efficiently from the heater to the ground. But once the bubbles are stopped, initial heat transfer conditions are recovered.

Finally, Figures 30 and 31 also confirm in a qualitative manner that the effects of the bubble injection are higher in the first experiment than in the second.

3 Quantitative analysis of the experiments

3.1 Resistance between the groundwater and the fluid: R_{gw-f}

A good indicator of the capacity of the bubbled groundwater to transfer the heat to the pipes is to calculate the thermal resistances inside the borehole.

Having experimentally obtained the temperature values of the secondary fluid (T_f) and the groundwater (T_{gw}), the thermal resistance between the fluid and the groundwater can be calculated with Equation 1.2. T_f is calculated as an average value (for both ways up and down) of the secondary fluid temperature in a specific borehole section. To calculate the power in each section, Equation 1.16 is used. The only incognita is then R_{f-gw}. Plotting the results:
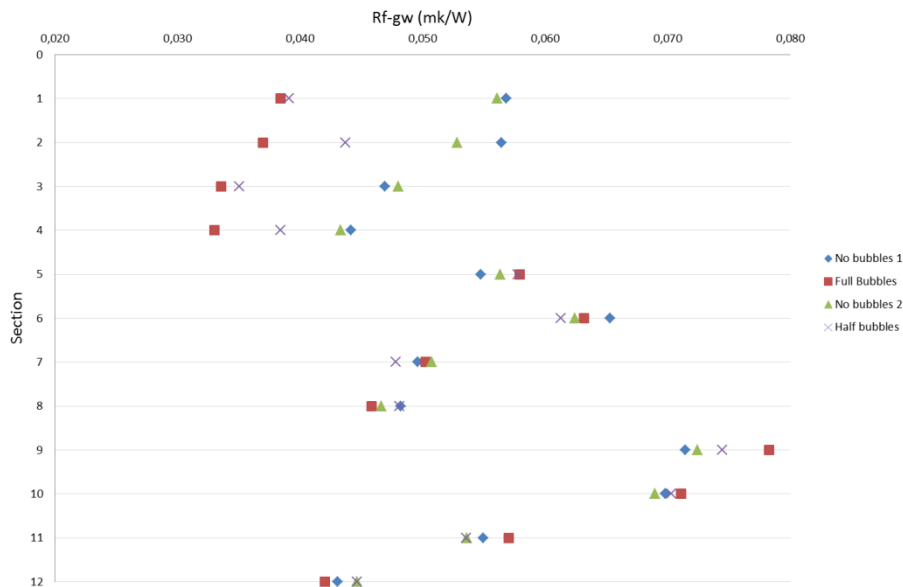
Figure 32: Representation of the Rf-gw in all sections for the two experiments and the recovery process

The resistances are clearly reduced in sections above the injection point (sections 1-4), where the reductions are between 40 to 55 % of the resistance without bubbles.

The R_{f-gw} is the sum of the convection between the secondary fluid and the pipes, the conduction inside the pipe walls and the convection between the pipe and the groundwater. In the case of bubbling, the reductions of the R_{f-g} are thanks to the enhancement of the convection between the groundwater and the U-pipe walls.

Moreover, the sizes of the bubbles also seem to have an impact on the convection with the pipe walls. As shown in Figure 32, the reduction of the values of the thermal resistances (as compared to the no bubble cases) increase in upper sections, where the bubbles are actually bigger.

In the case of half bubble injection, the resistances are 25-50 % lowered, also in the upper sections, with slightly smaller reductions compared to the case with full bubbles. Nevertheless, taking into account the amount of bubbles spent, the increase of convection between the groundwater and the pipe walls seems more efficient in the second experiment.

In sections located below the injection point, without the presence of bubbles, there are similar values of $R_{f\text{-}gw}$ with full, half and no bubbles. Therefore, there is no impact in the convection process between the secondary fluid and the groundwater in sections below the injection point.

3.2   Theoretical thermal rock conductivity

Although the convection in the groundwater side is not enhanced with the presence of bubbles below the injection point (chapter 3.1), the qualitative analysis done in chapter 2 show that the sections below the injection point are also thermally affected. When qualitatively observing the graphs of a fixed depth along the time (Figures 22 to 24), there is a sudden drop of the temperature of the groundwater in all sections. Moreover, in sections 5 to 12 there is a change of slope once the stationary conditions are achieved, possibly meaning a better heat transfer with the ground.

During steady-flux conditions, a change of slope in the groundwater side implies the same change of slope in the secondary fluid, and also to the borehole wall (the transient drops are finished, and stationary conditions mean that the temperature differences are constant in the different layers of the system). A change of slope in the temperature profiles of the groundwater means a change of behavior of the ground when absorbing the energy from borehole.

When analyzing the linear conduction model with the Equation 1.20, the temperature along the time has a logarithmic profile with a slope that is dependent on the rock conductivity (Equation 1.22). As the heater injects a constant rate of heat, the only parameter that modifies the slope in this model is the rock conductivity.

A graph has been plotted in every section to determine the logarithmic trend lines and the differences of slope between each experiment (no bubbles, half bubbles and full bubbles). In Figure 33, section 8 is represented, with the trend lines and its error represented for every experiment. The error R^2, measures the reliability of the curve fitting compared to the experimental data. R^2 ranges values from 0 to 1, being 1 the situation without error. Section 8 is a representation of what is done in the rest of the sections, which are all plotted in terms of an apparent thermal conductivity in Figure 34.
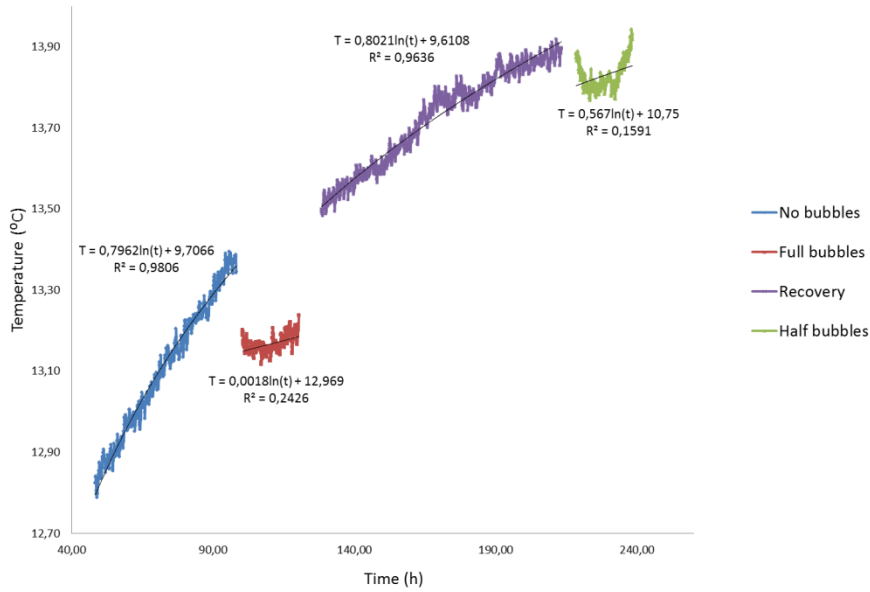
Figure 33: Representation of the logarithmic trend lines in every experiment for sector 8

The initial transient part of the curves in each experiment have not been taken into consideration, although it could be discussed how long this transition should be. The first analysis done in this chart is that the logarithmic approach of the data obtained has little error in the case without bubbles (less than two per cent error in the first no bubbles case, and 3.6% in the recovery), and thus it is a correct theoretical model to represent the dependence between temperature and time (as commonly done in thermal response tests).

Nevertheless, the model has an unacceptable error in the case of bubbles and half bubbles (with errors between 75 and 85 %), meaning that the logarithmic approach of Equation 1.15 may not be applicable in the situation with bubbles. This conclusion shows a change in the behaviour of the heat transfer mode in the ground, which may not only occur by conduction.

Various transition times have been studied and all of them agree with the main conclusion of this chapter: the logarithmic approach of the line-source model seems to be inappropriate. Given the relevance of this observation, further studies should be done regarding this statement in order to re-check if the results obtained by (Kharseh, 2010) regarding the effective thermal conductivity are valid. In the case of avoiding the first 15 hours of bubble injection, the model still presents an error between 75 and 85%.

However, it is clear from Figure 33 that the temperature increasing rhythm in the case of bubble injection is considerably decreased. As an approximation to know at what depths the heat is transferred in the ground, the linear model is used to calculate the rock conductivity using the slope of the logarithmic trend lines. The conductivity value changes show great dependence with the section.
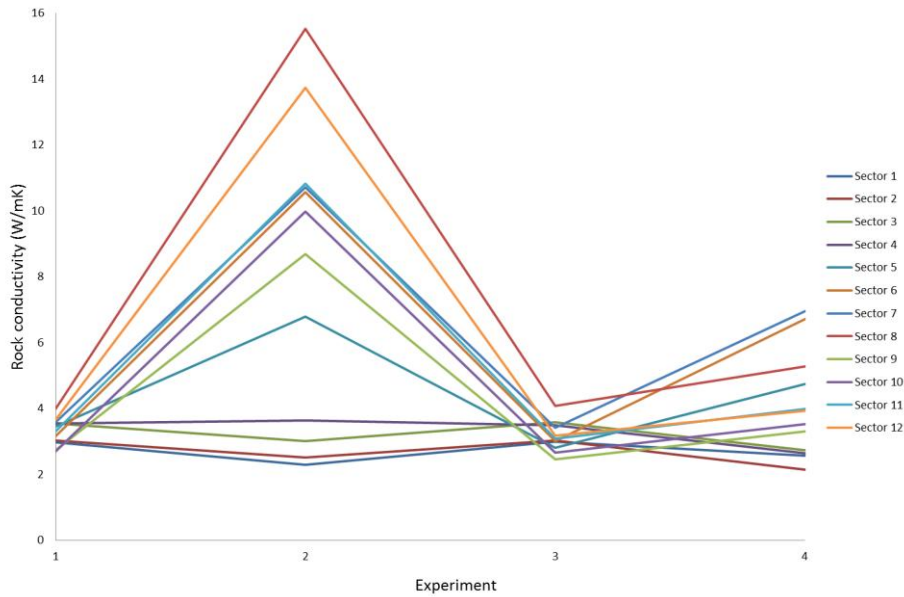
49

Figure 34: Rock conductivities values in the four phases of the DTRT in every section

First, the rock conductivity values in the case without bubbles are the only reliable ones, and they are very similar to the ones experimentally obtained by (Acuña J., 2010). On the other hand, the experiments with bubbles only give an idea of how the heat is better transferred along the ground.

In the case of bubbles the first 4 sectors do not detect a considerable change in the conductivity, but the rock conductivity in sectors 5-12 is clearly increased. When full bubble flow is compared to the situation without bubbles, sector 5 doubles its average rock conductivity and sectors 6, 7, 9, 10 and 11 triple their λ_{gw}. Sectors 8 and 12 result in values four times higher.

In the case of half bubbles, the effects are reduced to more than a half, although the increase of conductivity is also considerable.

As said previously, Figure 35 cannot be used to obtain real values of the rock conductivity in the case of bubbles, but the trend of the increasing values of the rock conductivity in sections below the injection point is relevant. Paradoxically, the sections above the injection point that had its thermal resistances reduced do not have an increasing of the conductivity. Therefore, the bubbles inside the groundwater do not seem to have a direct effect on the rock conductivity.

It is evident that the bubbles are indirectly responsible of this change of behaviour in the ground. The bubbles may be creating a motion in the groundwater side along the borehole, and not just above the injection point. Moreover, the introduction of bubbles inside the groundwater might raise the surface level of the groundwater. The increased movement of the groundwater and the disequilibrium of the surface level may involve a flow of groundwater coming inside and outside the borehole system. This movement of groundwater outside the borehole walls may affect the calculated conductivity of the rock, reducing the thermal resistance of the ground. On the other hand, this implication carries the inability to use the logarithmic approach of the line-source conduction model when the bubbles are injected.

3.3 Resistance of the borehole

If the linear conductive model is not applicable to the experiments with bubbles, the borehole thermal resistances cannot be calculated.

However, if the assumption of the validity of this model is done, the effects on the thermal resistances in every section can be compared. To carry this assumption, Equation 1.20 is used with constant conductivity values (obtained in the experiments without bubbles). Figure 35 compares the value of R_b depending on the section.
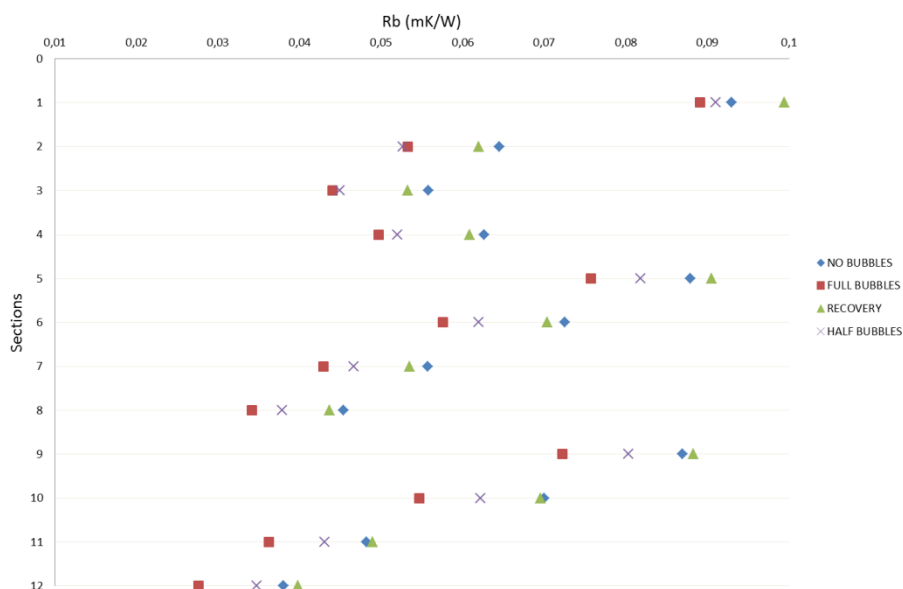

Figure 35: Borehole resistances in each section of the DTRT in every section

The reductions of the R_b along the borehole are constant. In the case of full bubble injection, the reductions are between 17 and 28 %, closely related to the values reported by (Kharseh, 2010). In fact, the reduction of thermal resistance in absolute numbers is very similar along the borehole, with values between $0.011 - 0.014$ mK/W.

In the case of the recovery period without bubbles, the resistances do not register any change. No effect of the previous bubbles in the borehole resistance is observed.

Finally, in the case of half bubble injection, the reductions of the R_b are between 7 - 20% of the initial values without bubbles. The values in the upper sections are very similar to the differences in the full bubble experiment. However, in the downer parts of the borehole, where there are no actual bubbles, the differences are bigger compared to the case with full bubbles.

This analysis quantifies the qualitative analysis done in chapter 2, when it was said that the effects of heat transferring seemed to be similar along the borehole. The linear model concludes that the borehole resistances decrease along the borehole in a similar rate. It also supports the conclusions of chapters 3.1 and 3.2: above the injection point the borehole resistance is enhanced, and below the injection point the heat transfer seems to be enhanced in the ground rock.

3.4 *"h"* coefficient in bubbled groundwater

This last chapter consists on a preliminary study of the *"h"* convection coefficient with the presence of bubbles in the groundwater. The main objective is to do a preliminary attempt of the coefficient calculation and to address future work in this field, more than obtaining accurate results.

As explained in the literature review, the *"h"* coefficient can be obtained from the Nusselt number. The use of the Groothuis and Handel correlation (Equation 1.11), allows the calculation of the Nusselt number from the Reynolds and Prandtl numbers.

The Reynold numbers depend on the fluid properties (that at the same time depend on the temperature of the fluid) and on the velocity of the fluid. The movement inside the borehole consists on air moving upwards accelerated and water filling the void space left by the bubbles. The assumption made to calculate the Reynolds number is that the air moves upwards with a constant speed (average value of the bubble speed), and that the water moves downwards with the same speed.

These assumptions limit the reliability of the results. The consideration of the same speed of the bubbles along the borehole rather gives an average value of the *"h"* coefficient. To be able to properly calculate the value of the *"h"* per section, the velocity of the bubbles and water should be accurately known in each sector. Apparently, this seems to be impossible as the approximation of calculating the speed of the water as a function of the bubble speed is an assumption itself. On the other hand, this assumption can be only applied to the points above the injection point, because under that point, there is no two-phase flow as the bubbles go upwards. However, the water might also have a turbulent movement.

It's been previously written that the average speed is u_m= 21,25m/min = 0,354 m/s. This speed corresponds to the average speed of the bubbles in the upwards direction, and the assumption is that the water also has the same speed in the other direction.

Moreover, the geometry needs to be specified in order to use Equation 1.11 and relate the Nusselt coefficient to the *"h"* coefficient. Therefore, a hydraulic diameter needs to be specified. In the case of the geometry studied, a pipe of a diameter of 140 mm and concentric pipes of a diameter of 42.4 mm. containing the secondary fluid, the hydraulic diameter is defined by (Javed, 2012) as:

$$Dh = Dbhw - \sqrt{2} \cdot Dp$$ Eq. 2.1

Where:

D_{bhw}... Diameter of the borehole wall

D_p... Diameter of the secondary pipe

Equation 2.1 leads a value of D_h=0.08 m.

The results of the theoretical calculations for *h* between the groundwater and the borehole walls range 2300-2900 W/$m^2 K$.

Experimentally, the *"h"* coefficient between the groundwater and the walls should be calculated with Equation 1.7 and the temperatures of the two substances in contact. Nevertheless, the temperature of the borehole walls is not directly calculated, and as the value of the borehole resistance can't be calculated (the linear model is not valid) there is no possibility of finding the *"h"* value experimentally.

However, the *"h"* convection coefficient between the groundwater and the secondary fluid pipes can be partly experimentally obtained from the thermal resistance between the groundwater and the secondary fluid (calculated in chapter 3.1). Calculating the convection between the secondary fluid and the pipes (R_{f-p}) and the conduction inside the pipes (R_p), the thermal resistance between the pipes and the groundwater (R_{p-gw}) can be obtained. Using the R_{f-p} and R_p values from (Acuña J. , 2010), the results for the *"h"* convection coefficient between the groundwater and the secondary fluid pipes range 250-6000 W/m^2K.

4 Conclusions

1   Visualization of the bubbles allowed evidencing the alteration of the conditions on the groundwater side and enabling the estimation of the bubble velocity along the borehole.

2   On the qualitative results during bubble injection, it is observed that the increase of temperature in time of the system decreases. Moreover, initial sudden drops of temperature along the depth are detected. The temperature profile shapes of the groundwater and secondary fluid along the depth significantly change during bubble injection. The difference between the secondary fluid and the groundwater temperatures decreases, implying a reduction of the thermal resistance. On the other hand, the asymmetry between the ways up and down in the temperature profile of the secondary fluid is increased, with only a 15% of the heat transferred in the way up. Finally, the homogenization of the temperatures in the groundwater side above the injection point indicates a reduction of the thermal resistance between the groundwater side and the borehole wall.

3   In the case of full bubble injection, the experimental thermal resistances between the secondary fluid and the groundwater above the injection point are decreased a 40-55%. This reduction is related to the better convection between the pipe walls and the groundwater. On the other hand, below the injection point there is no enhancement in the heat transfer. Moreover, the size of the bubbles affects the reduction of the thermal resistances: the bigger the bubbles are, the more enhanced the convection is.

4   When evaluating all the experiments along the time, the line source conduction model is not applicable to the case with bubble injection. When calculating the logarithmic trend line on the experimental data, the error in the case of bubble injection is 60-80%. Therefore, the results obtained through the model in the cases of bubble injection are not accurate (this applies to values of thermal conductivity and borehole resistance). In the case without bubbles, the model is confirmed to work properly. Even though the linear conduction model is not considered to be enough accurate in the experiments with bubbles, it has been used to calculate the rock conductivity and Rb values. These values are just used to make assumptions and/or to understand what parameters are enhanced, more than to quantify the values themselves.

5   The heat transfer in the ground is enhanced only in sections below the injection point. If the conductive linear model is used, the rock conductivity under the injection point increases abruptly depending on the section, possibly explained not as a conductive heat transfer improvement but as an increase of the heat transfer because of groundwater convection inside the bedrock. In sections above the injection point this effect is not visible.

6   When reducing the bubble injection flow to half, the thermal improvements are reduced compared to the case with full bubble flow. The thermal resistance between the fluid and the groundwater is reduced between 25-50%, a slightly lower reduction compared to the case with full bubbles (40-55%). The heat transfer in the rock is also increased considerably (considering the linear conductive model). To sum up, the reduction of the bubble flow does not have a great impact on the borehole thermal resistance reduction, but it does af-

fect the increasing of the heat transfer in the ground, as the experiments showed high dependence with the amount of bubbles used.

7   If the bubbles could be injected at the bottom of the borehole, the thermal resistance would be decreased along the whole depth, having more efficient thermal results. However, it is not sure whether it would increase the heat transfer in the rock. Other aspects like the pressurization requirements costs should also be studied in order to recommend a lower injection point depth.

8   The preliminary study of the convection heat transfer coefficient has been experimentally and theoretically calculated. Experimentally, the h coefficient between the pipes and the groundwater values varied a lot depending on the section, ranging values from 250-6000 W/m^2K. Theoretically, a Nusselt correlation with two-phase flow was used. There were several assumptions done, such as the velocity for the water being the same as the air bubbles average speed inside the groundwater. In this case, the average convection coefficient between the groundwater and the borehole wall is predicted to be around 2300-2900 W/m^2K.

5 Future work

As a consequence of some of the conclusions, I suggest some future work on the topic:

- A complete DTRT experiment with bubble injection to find a proper model that substitutes the conductive linear model in the ground. This model would enable the calculation of the borehole thermal resistance and the conductivity of the ground along the borehole.

- With the values of the borehole thermal resistance, find the "h" coefficient between the borehole wall and the groundwater. With the h values a Nusselt correlation could be proposed in relation with the speed of the bubbles at every specific depth.

- Analysis of the changes in the thermal borehole resistances and in the rock conductivity along the depth when injecting bubbles in different depths. Evaluate the cons of injecting the bubbles in such a low depth such as the costs of pressurizing the air.

- Optimization of the quantity of air used in the injection with several experiments with different amount of bubbles.

- Do a cost analysis of the bubbles spent and the benefits provoked by the thermal improvements.

References

Acuña, J. (2010). *Improvements of U-pipe Borehole Heat Exchangers.* Stockholm: KTH School of Industrial Engineering and Management, Division of Applied Thermodynamic and Refrigeration.

Acuña, J., Mogensen, P., & Palm, B. (2009). Distributed thermal response test on a U-pipe borehole heat exchanger. *Improvements of U-pipe Borehole Heat Exchangers* .

Bayer, P. e. (2012). Greenhouse gas emission savings of ground source heat pump systems in. *Renewable and Sustainable Energy Reviews , 16*, 1256– 1267.

Groothuis, H., & Hendal, W. P. (1959). Heat transfer in two phase flow. *Chemical engineering science , 11*, 212-220.

Gustafsson, A., & Gehlin, S. (2008). Influence of natural convection in water-filled boreholes for GSHP. *ASHRAE Transactions* , PART 1:416-423.

Incropera, F. (2007). *Fundamentals of heat and mass transfer.* New York: Willey.

Ingersoll, L. (1948). Theory of the Ground Pipe Heat Source for the Heat Pump. *ASHVE Transactions , 54*.

Javed, S. (2012). Thermal Model and evaluation of borehole heat transfer. *Chalmers university of technology, deppatrment of Energy and Environment* .

Johnson, H., & Abou-Sabe, A. H. (1952). Heat transfer and pressure drop for turbulent flow of air-water mixtures in a horizontal pipe. *QUE POSEM???*

Kharseh, M. (2010). Improve Thermal Characteristics of Borehole Heat Exchanger: Field Test and Analysis. *Swedish Patent (PCT/SE2010/050697)* .

Kim, D. (2002). Improved Convective heat transfer correlations for two-phase two-component pipe flow. *KSME International Journal , 16*, 403-422.

Monzó, P. (2011). Comparison of different Line Source Model approaches for analysis of Thermal Response Test in a U-pipe Borehole Heat Exchanger.

Nave, R. (2005). *van der Waals Equation of State* . Retrieved April 9, 2012, from Hyperphisics concepts, Department of Phisics ans Astronomy, GeorgaState University: http://hyperphysics.phy-astr.gsu.edu/hbase/kinetic/waal.html

Ociansson, W. (2011). *Energy Booster.* Karlstad: Patent och registreringsverket.

Omer, A. M. (2008). Ground Source heat pumps systems and applications. *Renewable and Sustainable Energy Reviews , 12*, 344–371.

Pletcher, R. H., & McMagnus , H. N. (1968). Heat Transfer and Pressure drop in horizontal anmnular two-phase, two-component flow. *Introd. Heat Mass Transfer , 11*, 1998-2001.

Sanner, B. e. (2003). Current status of ground source heat pumps. *Geothermics , 32*, 579–588.